UNIVERSITÉ DU QUÉBEC À MONTRÉAL

ESTIMATION DE LA RECHARGE DES EAUX SOUTERRAINES AU QUÉBEC MÉRIDIONAL PAR MODÉLISATION DE LA ZONE VADOSE ET LA SENSIBILITÉ AUX VARIABLES D'ENTRÉES

MÉMOIRE
PRÉSENTÉ
COMME EXIGENCE PARTIELLE
DE LA MAÎTRISE EN SCIENCES DE LA TERRE

PAR
SABRINA BRUNEAU

MARS 2020

REMERCIEMENTS

Je tiens d'abord à remercier les membres du comité de direction dont Florent Barbecot, Marie Larocque et Viorel Horoi pour l'opportunité et leur soutien au long du projet. Je voudrais remercier mon directeur Florent et Sophie Guillon pour m'avoir offert l'opportunité d'effectuer un stage en France qui fut une très belle expérience. Merci Marie pour ton soutien ainsi que pour la rigueur et la précision de tes révisions. Merci Viorel, toujours disponible pour m'aider lorsque j'en avais besoin en plus de ton implication dans l'infrastructure de recherche qui ne serait pas possible sans toi. Merci pour vos nombreuses initiatives nous permettant tous d'échanger lors de rencontres hebdomadaires tant au point de vue professionnel que personnel. L'opportunité de travailler au sein de grande équipe de recherche mêlant étudiants et chercheurs de tous les horizons est notamment un des aspects les plus enrichissants de mon expérience au cours de la maîtrise.

Je souhaite également remercier mes collègues avec qui j'ai partagé le quotidien pendant ces quelques années à l'UQAM. Ce passage a été enrichissant par l'entremise des projets auxquels j'ai pu participer, mais particulièrement grâce aux personnes formidables que j'ai rencontrées. J'aimerais tout particulièrement remercier Sylvain Gagné pour son temps et son implication d'une valeur inestimable au sein de l'équipe ainsi que Marjolaine qui m'a initiée à l'hydrogéologie et qui n'a jamais hésité à me donner un coup de pouce pour entamer mes propres travaux de recherche.

J'aimerais bien évidemment remercier ma famille et son support inégalable. Tout particulièrement mes parents d'amour qui m'ont permis de me rendre jusqu'où je suis aujourd'hui et pour qui je serai éternellement reconnaissante.

TABLE DES MATIÈRES

LISTE DES FIGURES

LISTE DES TABLEAUX

LISTE DES ABRÉVIATIONS, DES SIGLES ET DES ACRONYMES

AET	Actual evapotranspiration
ANUSPLIN	Australian National University Spline
GR	Groundwater recharge
IRRES	Infrastructure de recherche sur les eaux souterraines
K_s	Conductivité hydraulique à saturation
l	Paramètre de tortuosité et connectivité des pores
MAE	Mean Absolute Error
ME	Mean Error
NARR	North American Regional Reanalysis
NRCan	Natural Resources Canada
PET	Potential evapotranspiration
R^2	Coefficient de détermination

RMSE	Root Mean Square Error
SLZ	Saint-Lazare (site A et B)
STEL	Saint-Télesphore
S_y	Porosité efficace
T_{min}, T_{max}	Température minimale et maximale
VGM	van Genuchten-Mualem
VI	Vertical inflows
VWC	Volumetric water content
WTF	Water-table fluctuation
θ_r, θ_s	Teneur en eau résiduelle et saturée

RÉSUMÉ

La modélisation de la zone non saturée a reçu une attention grandissante dans la communauté scientifique au cours des dernières années afin d'estimer la recharge des eaux souterraines et d'étudier l'influence des différents facteurs contrôlant les processus inhérents. De plus, il a précédemment été démontré que les données d'humidité du sol peuvent fournir des informations utiles à la compréhension des processus d'écoulement dans la zone vadose. Dans cette optique, des données de teneur en eau du sol ont été enregistrées à trois sites faisant partie de l'infrastructure de recherche sur la recharge des eaux souterraines (IRRES) déployée dans la partie sud de la province de Québec au Canada. Ces données ont été subséquemment utilisées lors des processus d'inversion afin de calibrer le modèle HYDRUS-1D. Cette solution numérique basée sur l'équation de Richards a permis de quantifier et d'étudier les différents processus de recharge opérant dans la région d'étude, où l'eau souterraine est utilisée de manière croissante comme source d'approvisionnement en eau potable. Les teneurs en eau volumiques simulées somme toute représentent bien les données expérimentales sous différents couverts végétaux et types de sol. La proportion de matière organique et de silt semble jouer un rôle très important dans la caractérisation de la zone vadose afin de simuler l'écoulement particulièrement dans les premiers centimètres de profondeur. Les estimations de recharge de 2016 à 2018 démontrent des variations à travers les différents sites, variant entre 347 et 735 mm/an, dépendant principalement des schémas de précipitations et de la texture du sol au sein de la zone racinaire influençant directement la rétention de l'eau et les flux d'évapotranspiration. La recharge à long terme a par la suite été simulée avec les modèles calibrés fournissant de plus amples détails sur les relations entre les facteurs climatiques, les caractéristiques du sol et la recharge. Les résultats ont démontré que les variations interannuelles des flux de recharge sont fortement liées aux quantités de précipitations et leur distribution au long de l'année. Des périodes de recharge préférentielles distinctes ont été identifiées au printemps lors de la fonte, représentant 38 à 45% des précipitations, ainsi qu'à l'automne, représentant 29% des précipitations, suivant l'évolution de l'évapotranspiration potentielle et de la disponibilité en eau. Différentes sources de données météorologiques ont également été utilisées comme valeurs d'entrée du modèle dans l'optique de guider les futurs utilisateurs potentiels quant à la performance des différents jeux de données disponibles dans le sud du Québec.

Mots clés : eau souterraine, recharge, modélisation, zone non saturée, teneur en eau du sol, Québec méridional

INTRODUCTION

L'eau souterraine est une composante essentielle dans l'approvisionnement en eau potable des populations. Son utilisation est en croissance continuelle et permet actuellement d'approvisionner 20% de la population de la province québécoise sur près de 90% du territoire habité (MELCC, 2019b). Dans une démarche de développement durable, il est ainsi primordial d'établir des pratiques de gestion de l'eau souterraine qui limiteront les impacts anthropiques sur la ressource. Les principaux obstacles à l'élaboration d'une telle stratégie sont bien souvent le manque de connaissances et de données sur la recharge des eaux souterraines. À ce jour, la recharge demeure parmi les composantes du bilan hydrique les plus complexe à évaluer (Dripps *et al.,* 2007) puisqu'elle ne peut être mesurée directement et est grandement influencée par le climat, les hétérogénéités du sol et l'utilisation du territoire. Il existe de nombreuses méthodes pour estimer la recharge, par ailleurs aucune à elle seule ne permet d'obtenir une estimation fiable de la quantité d'eau qui recharge les aquifères souterrains (p. ex. profils isotopiques (Barbecot *et al.*, 2018), télédétection (Jackson 2002), balance de masse de chlore (Szilagyi *et al.*, 2011), water-table fluctuation (Crosbie *et al.,* 2005)). La précision et la fiabilité de ces méthodes reposent sur une variété de facteurs, dont les caractéristiques propres à chaque site (p. ex. le type de sol, la végétation, les conditions climatiques, la profondeur de la nappe phréatique, les hétérogénéités du sol) et de la disponibilité et la précision des données mesurées sur le terrain. La représentativité spatiale et temporelle des mesures expérimentales ainsi que la méthode utilisée afin d'en dériver des estimations requièrent également d'importantes considérations. De plus, puisque la recharge est généralement déduite à partir de mesures indirectes et à l'aide de modèles reposant sur un ensemble d'hypothèse simplifiant les processus naturels, de grandes incertitudes peuvent être associées à la quantification de la recharge. Il est ainsi primordial d'approfondir les connaissances vis-à-vis les différents processus générant la recharge en plus des facteurs qui les contrôlent pouvant varier d'une région à l'autre.

La modélisation de la zone vadose gagne en popularité grâce à de nombreuses démonstrations de sa capacité à fournir des estimations raisonnables de la recharge (Assefa *et al.*, 2013; Jiménez-Martínez *et al.*, 2009; Thoma *et al.*, 2014; Xie *et al.*, 2018) et s'est avérée pertinente dans l'évaluation du contrôle de différents facteurs (p. ex. caractéristiques hydrauliques du sol, conditions climatiques) sur les processus de recharge (Min *et al.*, 2015; Turkeltaub *et al.*, 2015; Wang *et al.*, 2014; Wang *et al.*, 2016). Ainsi, le modèle HYDRUS-1D a été utilisé dans la présente étude, afin de modéliser les processus dans la zone non saturée dans la région de Vaudreuil-Soulanges située dans le sud du Québec (Figure 1.1). Selon Larocque *et al.* (2015), l'utilisation de l'eau souterraine représenterait 30% de la recharge totale dans cette région où les activités agricoles dans les plaines argileuses sont importantes. La recharge serait également grandement localisée dans des zones spécifiques de dépôts perméables. L'emplacement stratégique des sites d'étude présentés a ainsi permis l'évaluation des flux d'eau souterraine dans ces zones préférentielles de recharge. Les résultats du modèle numérique de la zone non saturée ont été par la suite utilisés pour approfondir les connaissances sur le contrôle du climat et du sol sur la recharge dans la région d'étude.

La plupart des modèles hydrologiques et hydrogéologiques utilisent des données météorologiques en variables d'entrée afin d'en déduire des flux. La fiabilité des résultats sortants du modèle est ainsi fonction de la qualité de ces mêmes données. Par ailleurs, la disponibilité des jeux de données météorologiques et l'étendue de la distribution des stations climatiques sur le territoire demeurent actuellement d'importants facteurs limitants dans le cadre de nombreux projets. Afin de résoudre ce problème, plusieurs produits climatiques sur grille ont été développés au courant des dernières années rendant disponibles des données météorologiques d'une grande variété de résolutions spatiales et temporelles. La comparaison de ces différents produits doit par la suite être effectuée afin d'en évaluer la fiabilité au sein de chaque région ainsi qu'être incorporée dans les modèles hydrogéologiques pour évaluer leur impact subséquent sur les résultats de simulation (Choi *et al.*, 2009; Langlois *et al.*, 2009). À cet effet, deux produits météorologiques sur grille ont été évalués pour en déterminer la fiabilité à reproduire les conditions climatiques observées dans la région de Vaudreuil-Soulanges durant la période d'intérêt. Les erreurs associées avec chaque produit ont été par la suite examinées lors de leur incorporation dans le modèle numérique en données d'entrées afin d'évaluer l'incidence sur l'estimation de la recharge résultante.

Le projet de recherche présenté cherche à améliorer notre compréhension de la dynamique ainsi que des processus qui sont responsables de la recharge des aquifères par l'entremise des objectifs suivants : (i) estimer la recharge en utilisant un modèle de la zone non saturée basé sur l'équation de Richards dans un aquifère au sud de la province de Québec (ii) analyser les différents processus et facteurs qui contrôlent la recharge (iii) quantifier les différences entre deux produits météorologiques disponibles publiquement et (iv) quantifier les erreurs associées aux estimations de recharge associées aux différents produits climatiques utilisés.

La principale originalité de ce projet de recherche réside dans l'utilisation en méthode inverse d'un modèle de simulation 1D des transferts d'eau dans la zone non saturée pour l'estimation de la recharge en contexte québécois. Ces résultats sont importants pour le champ disciplinaire concerné, soit l'hydrogéologie, notamment à ce qui a trait aux données météorologiques pouvant être utilisées dans l'estimation de la recharge des aquifères. Cette étude permettra ainsi de fournir des estimations raisonnables de la recharge des eaux souterraines au sein des zones préférentielles de recharge dans la région d'étude en plus d'une reconnaissance notamment du contrôle du climat et des caractéristiques du sol sur les processus de recharge. Les résultats pourront également démontrer l'importance du choix des produits météorologiques en données d'entrées quant à leur influence sur la quantification de la recharge.

Le mémoire a été écrit sous forme d'un article scientifique qui sera soumis à la revue *Journal of Hydrology : Regional Studies*. Le coeur de l'article a donc été produit selon les directives de la revue et a été rédigé en anglais.

CHAPITRE I

SIMULATION OF GROUNDWATER RECHARGE IN SOUTHERN QUEBEC BY VADOSE ZONE FLOW MODELING AND ITS SENSITIVITY TO INPUT VARIABLES

Sabrina Bruneau[1,2*], *Florent Barbecot*[1,2], *Marie Larocque*[1,2], *Viorel Horoi*[1]

[1] Département des sciences de la Terre et de l'atmosphère - Université du Québec à Montréal, C.P. 8888, Succ. Centre-Ville, Montréal (QC), Canada, H3C 3P8

[2] GEOTOP Research Center - Université du Québec à Montréal, C.P. 8888, Succ. Centre-Ville, Montréal (QC), Canada; tel: 514-987-3000 ext. 1515; fax: 514-987-7749

ABSTRACT

Increasing attention has been given to vadose zone modeling in order to estimate groundwater recharge (*GR*) and to better understand the impacts of different controls on recharge processes. In addition, the volumetric water content time series have previously demonstrated to be valuable information to study the vadose zone. Therefore, soil moisture data monitored at three sites from the Groundwater Recharge Research Infrastructure (IRRES) in southern Quebec province Canada, were used to calibrate the HYDRUS-1D model. The numerical solution based on Richards equation permitted to quantify and identify important factors for simulating the near-surface water balance in the region of interest where groundwater is increasingly used as a source of fresh water. The simulated soil moisture contents generally well matched the experimental data under varying vegetation and soil conditions. The organic matter content and silt fraction seemed to play an important role in the soil moisture behavior particularly in the first few centimeters depth. The resulting *GR* estimates from 2016 to 2018 showed variations across sites, ranging between 347 to 735 mm/year, depending mostly on precipitation patterns and soil texture in the root zone controlling soil water retention and evapotranspiration. The subsequent long-term recharge estimation with the calibrated model provided further insights of the relationship between climate factors, soil characteristics and *GR*. The results showed that the inter-annual variations in *GR* are largely dependent on precipitation quantity and distribution all along the year. The monthly recharge patterns have also been examined with distinct preferential recharge periods in spring snow melt, representing 38 to 45% of precipitation, and in fall, representing approximately 29% of precipitation, following potential evapotranspiration patterns and the availability of water. Different

meteorological datasets have been used as input values to the model in the attempt of providing guidance to potential users regarding the performance of different meteorological datasets in southern Quebec province for hydrogeological modeling.

Keywords: groundwater, recharge, modeling, unsaturated zone, soil moisture content, southern Quebec

1.1 Introduction

Groundwater is a renewable resource, however, it is essential to establish sustainable groundwater management to limit anthropogenic impacts on this resource. The lack of knowledge and data on *GR* represent an important obstacle to a successful management strategy. To these days, this component is still extensively considered as one of the most challenging water-balance components to quantify (Dripps and Bradbury, 2007) since it cannot be measured directly and it is strongly influenced by climate, soil heterogeneity and land uses. Despite the development of numerous methods in previous studies, no single method provides a reliable assessment of the quantity of water actually replenishing the aquifer (e.g., isotopic profiles (Barbecot et al., 2018), remote sensing techniques (Jackson 2002), chloride mass balance (Szilagyi et al., 2011), water-table fluctuation (Crosbie et al., 2005)). The accuracy and reliability of those methods depend on a variety of factors, including mainly site characteristics (e.g., soil type, vegetation, climate conditions, water-table depth, soil heterogeneity) and the availability and accuracy of field data (Scanlon et al., 2002). The representativeness of the spatial and temporal scales by the field measurements used to derive estimates also require important consideration. It is thus of high importance and interest to better understand the different recharge processes in addition to factors controlling them in each specific region.

In recent years, vadose zone modeling has gained popularity because of its demonstrated capacity to offer reasonable *GR* estimates (Assefa et al., 2013; Jiménez-Martínez et al., 2009; Thoma et al., 2014; Xie et al., 2018) and was useful in the control assessment of different factors (e.g., soil hydraulic characteristics, climatic conditions) on *GR* processes (Min et al., 2015; Turkeltaub et al., 2015; Wang et al., 2014; Wang et al., 2016). Therefore, the model HYDRUS-1D has been used in this study in order to simulate recharge processes in the unsaturated zone in Vaudreuil-Soulanges region located in southern Quebec, Canada (Firgure 1.1). It has been estimated by Larocque et al. (2015) that the groundwater use represents 30% of the total recharge in this area where agricultural activities are dominant in the clayed lowland. In addition, *GR* is highly localized in particular zones of permeable sediment deposits. The location of the study sites enables the evaluation of groundwater flow in those preferential recharge zone of the Vaudreuil-Soulanges region. The results from the unsaturated numerical model were further used to deepen the knowledge of climatic and soil controls on *GR* in the studied region.

In addition, the availability of meteorological datasets or the sparse distribution of climate stations remain limiting factors in numerous studies. To resolve this issue, several gridded climate products have been developed in the past years allowing the availability of meteorological data on varying range of temporal and spatial resolution. Therefore, the comparison of the different datasets must be performed to evaluate their reliability and be incorporated in hydrogeological models to evaluate their subsequent impact on the simulations (Choi et al., 2009; Langlois et al., 2009). In this regard, two gridded meteorological products have been evaluated to determine their reliability in reproducing observed climate conditions in the Vaudreuil-Soulanges region over the period of interest. The errors associated with each dataset were further examined through their incorporation in the numerical model to evaluate the impact of their individual discrepancies on the resulting *GR* estimation.

Therefore, the objectives of this research are (i) to estimate recharge using a vadose zone model based on Richards equation in a southern Quebec aquifer (ii) analyse the different processes and factors controlling recharge (ii) to quantify the differences between two publicly available meteorological datasets and (iii) to quantify the discrepancies associated with the resulting recharge estimates.

The main originality of this study resides in the utilization of inverse modeling method for 1D simulations of water transfer within the unsaturated zone in order to estimate *GR* in Canadian context. Those results are important for the concerned disciplinary field concerning the meteorological data that can be possibly used for *GR* estimation. This study will provide reasonable estimations of *GR* in the preferential recharge areas in the study region in addition to the acknowledgement of the control of climate and soil characteristics in the recharge processes. Those results will also demonstrate the importance of choosing the appropriate meteorological product as input data due to their influence on recharge quantification.

1.2 Study Area

The study area is located in the region of Vaudreuil-Soulanges, near the boundary between Ontario and the United States (Figure 1.1). It is part of the Groundwater Recharge Research Infrastructure (*Infrastructure de recherche sur la recharge des eaux souterraines* - IRRES), which consists of *GR* monitoring stations distributed in southern Quebec (Canada). In the Vaudreuil-Soulanges region, it has been estimated that 20 million cubic meters of water is consumed each year from which 54% is from groundwater and 46% from surface water (Larocque et al., 2015). This percentage is significantly higher than the proportion of groundwater use of 20% estimated for the whole province (MELCC, 2019b)

1.2.1 Geology and hydrogeology

Clay soils are dominant in the lowland portion of the Vaudreuil-Soulanges region and are occupied by agricultural land that covers 63% of the territory. Those clay of marine origin can reach a thickness of up to 30 m and significantly limit *GR* for the whole region. It was estimated by Larocque et al. (2015) with a spatial surface water budget, that *GR* can range from 0 in clayed lowlands to a mean maximum of 440 mm/year in permeable areas in the Vaudreuil-Soulanges region. At the location of the Saint-Telesphore esker, Saint-Lazare and Hudson hill, well drained and thick fluvioglacial deposits represent highly permeable granular aquifers and preferential recharge zones (Larocque et al., 2015). It is estimated that the Hudson and Saint-Lazare hill receive a mean annual recharge rate of 356 mm/year, which represents 41% of total regional recharge. Other fluvioglacial deposit areas of smaller extend, including the unconfined part of Saint-Telesphore esker, receive a mean annual recharge of 256 mm/year. Aquifer recharge occurs in episodic events, mostly in the fall (October to December) and during the spring snow melt (March to May).

The topography varies across the extent of the region with a slope varying between 0 and 63° with a mean of 1°. In the clay lowland, the hydraulic gradient is small (10^{-3} m/m) where the groundwater flux is towards the south and south-west from the high topographic levels representing key recharge zones. At the eastern extremity of the clay lowland, groundwater flows are in eastward direction. In the northern part of the Vaudreuil-Soulanges region, the groundwater flow is mostly in the northward direction from the high topographic levels associated (mount Rigaud, Saint-Lazare and Hudson Hill), with high hydraulic gradient (4×10^{-2} m/m on mount Rigaud hillsides).

1.2.2 Instrumented sites

The Saint-Telesphore (STEL) site lies on fluvioglacial sandy deposits reaching up to 40 m thickness above the regional bedrock aquifer and 86 m on Saint-Lazare (SLZ) hill. The latter is composed of thick and complex fluvioglacial deposits that were reworked on the surface and now characterized as deltaic and littoral glaciomarine deposits. Depending on the energy regime and the progression of the ice margin, the fluvioglacial deposits on SLZ hills are represented as silty beds or with the presence of blocks in the first meter depth. Those thick fluvioglacial deposits lay on a discontinuous and variable beds of till and ancient quaternary sand before reaching the sandstone bedrock. This highly variable spatial distribution of sediments leads to the repartition of confined and unconfined conditions for the deep aquifer on SLZ hill while the aquifer at STEL site is locally unconfined.

There are two stations at the Saint-Lazare site to evaluate the effect of vegetation on the water flux dynamic. The first one is located in a forest outcrop covered with a sparse grass (SLZA) and the other site, at a 15 m distance, is located in a jack pine forest (SLZB). A third site has been installed at STEL and includes a weather station. The vegetation in the area of STEL is mainly represented by woodland, aside from the site outcrops next to a sand quarry dominated by dense prairie grass land cover and where the unsaturated zone was studied. At those three locations, well drained sandy soils are dominant at the surface with hydraulic conductivity on the order of 10^{-5} to 10^{-4} m/s according to field experiments using Guelph Permeameter (Soil Moisture Equipment Corp, 2013). The thickness of the vadose zone at the study sites varies between 4.8 to 7.4 m and the average water table depth is located at 5.5 and 6.8 m below the surface at SLZ and STEL, respectively.

Piezometers (2 inches diameter) instrumented with level loggers (Solinst) were installed at the two sites. The borehole at SLZ was drilled in September 2015 and is

8.5 m deep. The sediments were characterized as medium to fine sand uniformly distributed through the soil column. At STEL the borehole was drilled in August 2013 and the sediments are fine to medium sand from 0 to 4.1 m, silty clay between 4.1 to 6.5 m, and again fine to medium sand from 6.5 to 10 m. Below, the sediments vary between coarse and fine medium sand down to 21.6 m.

1.2.3 Meteorological conditions

The 1981-2010 climate normal means for three weather stations in the region (MELCC, 2019a), report a mean annual air temperature of 6.3°C with a maximum of 11.1°C and a minimum of 0.6 °C. The mean total annual precipitation is 980 mm of which 16% falls as solid precipitation.

1.3 Materials and methods

1.3.1 Site instrumentation

Soil moisture was measured at the three experimental sites from 2015 to 2018 (Table 1.1). Soil volumetric water contents (VWC) were measured with capacitance sensors (model EC-5, Campbell Scientific Inc.) every 15 minutes and then integrated to daily values.

The weather station at STEL is equipped with various measurement devices to collect basic meteorological data every 15 minutes (all at 2 m height except for the anemometer located at 3 m). The incoming solar radiation was measured with a Kipp & Zonen Pyranometer SP LITE2 and the net radiation was measured with Kipp & Zonen Net Radiometer Sensor NR-LITE2 with both a temperature range between -40° to 80°C. Wind speed and direction were available through a Young Wind Monitors 05103-45 anemometer with the accuracy of ± 0.3 m/s. The air temperature and relative humidity were recorded with a Campbell Scientific HMP60 probe with the accuracy of ± 0.6°C at an operating temperature range between -40° and +60°C and an accuracy varying between 3 and 7% for the relative humidity depending on the air temperature. The groundwater level at both sites was monitored hourly by automatic transducers in instrumented piezometers installed in a granular unconfined aquifer with levelogger Solinst 3001 M5. Lastly, precipitation was measured using a Hydrological Services Tipping Bucket Rain Gauge with a funnel extension for snowfall measurements. There is no information on the precipitation phase because the measurements are the equivalent precipitated amount of water. The separation between liquid and solid precipitation was calculated as a function of maximum and minimum air temperature from the equation of Fortin and Turcotte (2007) as follows:

$$if\ T_{max} \leq 0°C,\ \ SnowFrac = 1 \qquad \text{(eq. 1)}$$

$$if\ T_{min} \geq 0°C,\ \ SnowFrac = 0$$

$$else\ \ SnowFrac = 1 - \frac{T_{max}}{T_{max} - T_{min}}$$

where T_{min} and T_{max} are daily maximum and minimum temperature (°C) and *SnowFrac*, the snow fraction for the daily precipitation events.

1.3.2 Site characterization

Soil cores were sampled at different depths at each site. Soil samples were retrieved in spring 2019 at STEL from 10, 20, 40, 60 and 90 cm depth and at SLZ in summer 2018 at 20, 40, 55, 90 and 115 cm for grain size analysis by laser sieving. The physical description of the textural group which the samples belongs to is based on Folk (1954). The gravel fraction was mostly under 1% with a maximum of 4% at STEL from the soil sample at 60 cm depth. The organic matter content was estimated by ignition loss (Dean, 1974; Heiri et al., 2001).

1.3.3 Water-table fluctuation method

It is well known that uncertainties exist among all the available techniques for estimating *GR* (Scanlon et al., 2002). It is crucial to evaluate the reliability of *GR* to quantify the potential variability of *GR* at the IRRES sites using multiple techniques. The simulated *GR* are thus compared to the results obtained from the water-table fluctuation (WTF) method (Healy and Cook, 2002). The latter has been used in numerous studies due to its simplicity and its low data requirement (Crosbie et al., 2005; Delin et al., 2007; von Freyberg et al., 2015). Because this method does not rely on meteorological data as input, it is especially useful for comparison with the model results. The WTF method is used to estimate *GR* based on water-level fluctuation data and requires knowledge of the aquifer specific yield (*Sy*). This method is based on the assumption that rises in groundwater levels in unconfined aquifers are due to water reaching the water table and recharging the aquifer. It assumes that the amount of available water in a column of unit surface area is *Sy* times the height of the water in the column. The comparison of estimates from different methods will give insights in the hydrogeologic processes taking place at the studied catchment.

1.3.4 Available meteorological data

Daily atmospheric data were retrieved from different publicly available sources and compared with measurements from our weather monitoring station. Meteorological data were available from three different sources (Table 1.2). First, the automated weather station located at STEL site records local air temperature, precipitation, solar radiation and wind speed. Secondly, observed data of daily minimum and maximum temperature (T_{min}, T_{max}) and precipitation interpolated on a 10 km grid by Natural

Resources Canada (NRCan) based on the Australian National University Spline (ANUSPLIN) interpolation method (Hopkinson et al., 2011; Hutchinson et al., 2009; McKenney et al., 2011) are also available. Finally, daily temperature, precipitation, radiation, albedo and wind speed data are available from the North American Regional Reanalysis (NARR) atmospheric and land surface hydrology dataset, which uses the very high resolution NCEP ETA Model together with the Regional Data Assimilation System (Mesinger et al., 2006). As the daily T_{min} and T_{max} of NARR were not available, the minimum and maximum values of daily temperature were derived from the 3-hourly data.

The added value of using NARR and ANUSPLIN data were investigated through hydrological modeling at the STEL station chosen for the case study. Three different runs with varying configurations of the ANUSPLIN and NARR datasets as input weather data were performed for the period 2016-2018. The first run, referred to as *ANUSPLIN scenario* and employs T_{min}, T_{max} as well as precipitation from ANUSPLIN database. The missing terms (e.g., radiation) were estimated with temperature or were set constant (wind speed set to 2 m s^{-1} and albedo set to 0.23 for grass; see Allen et al. (1998) for more details). The second run, denoted *NARR scenario* and comprises T_{min}, T_{max}, precipitation, radiation terms, albedo as well as wind speed from reanalysis meteorological data NARR. The third run incorporates data from both datasets, i.e. T_{min}, T_{max} and precipitation from ANUSPLIN and all the other variables from NARR and will be denoted *combined scenario*. The latter represents a more complete dataset that maximises the number of available variables for *GR* modeling. Because the ANUSPLIN data for 2018 were not available at the time of the study, temperature and precipitation were taken from the STEL weather station for that year, because those two variables were very well correlated within the data source.

Due to temporal discontinuities in the STEL dataset, it was only used for comparison purposes to evaluate the accuracy of NARR and ANSUPLIN datasets. The comparison was made against measurements from a weather station that includes main meteorological variables (temperature, precipitation, radiation and wind speed) needed for the calculation of potential evapotranspiration (*PET*).

A degree-day model was used to assess daily snow melt available for infiltration corresponding to the following equation:

$$Melt = \begin{cases} C_{melt} \times (T_{air} - T_{melt}), & T_{air} > T_{melt} \\ 0, & T_{air} < T_{melt} \end{cases} \qquad \text{(eq. 2)}$$

where *Melt* is daily snow melt (mm/day), C_{melt} represents the snow melt coefficient (mm/°C/day), T_{air} is the mean daily air temperature (°C) and T_{melt} the temperature at which the snow starts to melt and was set to 0°C. The snowpack density and depth were retrieved from the MELCC (2019a) nearby meteorological station to calibrate the snow melt coefficient from the degree-day model and simulate the evolution of the snowpack during the winter seasons from 2000 to 2017. The daily calculated values of snow melt are added to the liquid fraction of daily precipitation to generate vertical inflows values (*VI*).

1.3.5 Model setup and parameterization

Once water reaches the ground, an amount is loss by evaporation and the remaining quantity entered the soil. It migrated through the unsaturated zone to increase the soil moisture storage, where a large portion of the water is going back to the atmosphere by plant uptake or drained through the root zone to recharge the aquifer.

The physically based vadose zone model HYDRUS-1D (Šimůnek, J. et al., 2013) was used in this study. Based on the Richards equation, the model enables the simulation of soil moisture dynamics within a soil column representing the unsaturated zone. The drainage through the root zone leaving the base of the soil column is taken as *GR*. The van Genuchten-Mualem (VGM) model (Mualem, 1976; Van Genuchten, 1980) was chosen as a model to represents, by continuous mathematical function, the water retention characteristics and the hydraulic conductivities of soil in the given samples:

$$\theta(h) = \begin{cases} \theta_r + \frac{\theta_s - \theta_r}{(1+|\alpha h|^n)^m}, & h < 0 \\ \theta_s, & h \geq 0 \end{cases} \qquad \text{(eq. 3)}$$

$$K(S_e) = K_s \times S_e^l \times \left[1 - \left(1 - S_e^{1/m}\right)^m\right]^2 \qquad \text{(eq. 4)}$$

where θ [L^3/L^3] is volumetric moisture content; h [L] is pressure head; θ_r and θ_s are residual and saturated moisture content respectively; K [L/T] and K_s[L/T] are unsaturated and saturated hydraulic conductivity, respectively; and $S_e = (\theta - \theta_r)/(\theta_s - \theta_r)$ [-] is saturation degree. For the fitting factors, α [1/L] is inversely related to the pressure at the inflexion point of the retention curve, n [-] measures the pore size distribution of a soil with m = 1- $1/n$, and l [-] is a parameter accounting for pore tortuosity and connectivity.

The initial VGM parameters (θ_r, θ_s, K_s, α and n) were estimated using the ROSETTA software (Schaap et al., 2001). ROSETTA uses pedotransfer functions to predict the VGM parameters using the soil textural distributions that were obtained from laboratory analyses for the three study sites. The saturated hydraulic conductivities (K_s) were set to field-measured values when available and the pore-connectivity parameter l was set to an initial value of 0.5 corresponding to an average value for many soils (Mualem, 1976).

An atmospheric upper boundary condition was selected at the surface of the modeled soil columns. Surface runoff was considered inexistent because the slope at both sites is very gentle and the three stations are covered by permeable sediments that limit runoff. A free drainage was set at the base of the soil column as a lower boundary condition. The length of the modeled soil columns was set at 3 m with a total of 301 nodes evenly distributed between the surface and bottom. The daily *PET* rates were calculated with the Penman-Monteith equation (Allen et al., 1998), which was then used along with daily *VI* values to drive the vadose zone model. Beer's law was used to partition *PET* into potential evaporation (E_p) and transpiration (T_p) directly into the model:

$$E_p(t) = PET(t) * e^{-k*LAI(t)} \quad \text{(eq. 5)}$$

$$T_p(t) = PET(t) - E_p(t) \quad \text{(eq. 6)}$$

where k is an extinction coefficient and *LAI* is leaf area index (L^2/L^2). *LAI* data were obtained from MODIS_MCD15A3H dataset with spatial resolution of 500 m x 500 m at 4-days intervals (Myneni et al., 2015). The daily *LAI* data at each site were obtained by linear interpolation between the 4-days coupled with a moving average of 30-days window. *LAI* was used as a primary factor controlling the difference in *PET* among different ecosystems in the same ecozone, such as the forest and the pasture (Zha et al., 2010). Therefore, *LAI* data at SLZ site were extracted from two close points from the site but with each representing better their respective ecosystem (forest and grassland). The root water uptake was computed using the Feddes et al. (1978) model:

$$S(h) = \alpha(h) * S_p \quad \text{(eq. 7)}$$

where $\alpha(h)$ is a dimensionless function varying between 0 and 1, depending on soil matric potential, and S_p [1/T] is the potential root water uptake and assumed to be equal to T_p. The distribution of S_p over the root zone depends on root density distributions (between 0 and 1) attributed to each site and was selected based on field observations and literature descriptions of vegetation physiological characteristics. In a 3m-deep sandy soil cores analyzed for root biomass by Wang et al. (2009b) in grassland environment, 60-70% of the total root mass occurred in the top 20 cm depth. At STEL and SLZA sites, the root density was linearly distributed from 1 at the surface to 0 at a depth of 30 cm. The Jack pine trees generally develop lateral root system spreading to at least 8.5 m and the bulk of the root system is largely confined in the upper 45 cm of the soil and mostly in the top 15 cm (Rudolph, 1985). Therefore, at SLZB site the root density was equal to 1 from 0 to 30 cm and a density varying from 1 to 0 was distributed to up to a depth of 45 cm. The root water uptake was then assumed to be equal to actual transpiration. The actual evapotranspiration (*AET*) was the sum of actual soil evaporation and actual transpiration rate. The parameter values for delineating root water uptake were taken from the database integrated into HYDRUS-1D model and assigned as alfalfa. It has to be noted that the interception has not been considered due to the lack of data and parameter values.

1.3.6 Model calibration

The soil hydraulic parameters (θ_r, θ_s, α, n, l and K_s) were calibrated automatically using the Marquardt-Levenberg type parameter optimization algorithm (Marquardt, 1963) implemented in the HYDRUS-1D model. The calibration period excludes winter months (January to March) and was conducted from 2016 to 2018, covering three years of contrasted meteorological conditions with 2015 taken as a spin-up period to minimize the effect of initial conditions. The simulated soil columns were divided into four layers given the depth of each soil moisture sensors. The calibrated parameters were used afterward to simulate the long-term recharge estimates from 2004 to 2017 with the year 2003 as the spin-up period. To evaluate the impact using auxiliary datasets on *GR* estimates, the calibrated model at STEL site was run from 2016 to 2018 with the three meteorological scenarios described above.

Three performance criteria were selected to evaluate the goodness-of-fit of the model results, including (i) Root Mean Square Error (RMSE), a measure of the average difference between modeled and observed results. Smaller RMSE indicates better prediction of the model; (ii) Mean Error (ME) and Mean Absolute Error (MAE), a measure of the bias of the modeled results compared to observed values inform of an over-prediction or under-prediction of the model; (iii) coefficient of determination (R^2), a measure of the agreement between observed and modeled results. A value of 1 suggests a perfect correlation between the fitted and observed values.

$$RMSE = \sqrt{\frac{1}{n}\sum_{i=1}^{n}(P_i - O_i)^2} \quad \text{(eq. 8)}$$

$$ME = \frac{1}{n}\sum_{i=1}^{n} P_i - O_i \quad \text{(eq. 9)}$$

$$MAE = \frac{1}{n}\sum_{i=1}^{n}|P_i - O_i| \quad \text{(eq. 10)}$$

$$R^2 = \frac{\left[\sum_{i=1}^{n}(P_i-\bar{P})(O_i-\bar{O})\right]^2}{\sum_{i=1}^{n}(P_i-\bar{P})^2\sum_{i=1}^{n}(O_i-\bar{O})^2} \quad \text{(eq. 11)}$$

P_i and O_i represent predicted and observed values respectively while $\bar{P}$ and $\bar{O}$ are average values of the predicted and observed time series.

1.4 Results and discussion

1.4.1 Comparison of meteorological datasets

Prior to using NARR and ANUSPLIN data to drive the vadose zone model, a comparison of the datasets with ground-based measurements from STEL was performed. Figure 1.2 shows the results from the comparison of mean daily air temperature, cumulative annual precipitation and net radiation for the period of 2016 to 2017 for ANUSPLIN and up to 2018 for NARR. There were several days with missing records at the STEL station and, for the purpose of consistency, days with missing observations were excluded from each dataset in the statistics. Note that the net radiation for ANUSPLIN has been calculated from temperature data.

Strong correlation between the datasets has been found especially for temperature data with a R^2 of 0.99 and a slope of 1 for ANUSPLIN and is more scatter in the NARR data with a R^2 of 0.95 and a slope of 0.98 (Figures 1.2a and 1.2b). The precipitation data from ANUPSLIN have a very similar distribution compared to the measurements made at the station in 2017 (Figures 1.2c and1.2d) and exhibit similar results for 2016 (not shown here). A significant bias was observed for NARR precipitation data producing a substantial underestimation in annual values. Another grid point has been extracted from NARR dataset near the study site to test the hypothesis of an inaccurate point grid, but similar results were found. This might be attributed to the unavailability of gauge precipitation observations over Canada, therefore no precipitation is assimilated since 2003 over the country (Mesinger et al., 2006). The agreement between the net radiation from the NARR dataset and from the values measured at STEL is acceptable (R^2 = 0.82 and slope = 1.01) and of lower agreement for the calculation of net radiation from temperature values (R^2 = 0.77 and slope = 0.95) (Figures 1.2e and 1.2f). Both net radiation comparison results show an overestimation particularly during summer months. The overestimation of radiation by the reanalysis dataset may be explained by the uncertainty linked to the extracted data for a specific location from the relatively coarse (32 km) grid of this dataset (e.g., cloud cover fraction and forest cover limiting solar exposition).

Langlois et al. (2009) used NARR meteorological data to drive three multilayered thermodynamic snow models in southern Quebec. They compared the meteorological station measurements at Sherbrooke University (45.378N, 71.928W) with NARR data for winter periods from 2004 to 2008 and found a reasonable agreement. In the

Langlois et al. (2009) study, the simulations of snow water equivalent gave better results with NARR data as input instead of the ground-station data, for a particular year, due to improper precipitation data monitored at the meteorological station (instrumentation problems). In addition, Wong et al. (2017) inter-compared several gridded precipitation products over 15 terrestrial ecozones in Canada for different seasons from 1979 to 2012 at a 0.5° and daily spatio-temporal resolution. The overall reliability of NARR demonstrated the lowest quality because of the non-assimilation of gauge precipitation. Therefore, they reported that ANUSPLIN performed well in capturing the timings and minimizing the error magnitude of the precipitation. Due to the limitations in the various meteorological observations, the combination of multiple data sources has been undertaken in other studies (Maggioni et al., 2014; Shen et al., 2010). Therefore, the combined scenario was used to calibrate the vadose zone models to study the *GR* processes operating at the IRRES stations.

An overview of the hydroclimatic conditions across the study area is given as a statistical summary of annual mean *VI* at *PET* at each site. Both wet and dry years were encountered during the calibration period. The year 2017 is characterized as a wet year with significant amount of precipitation (926-1014 mm) coupled with an early snow melt (mid-February) leading to important flooding events in southern Quebec (NASA, 2017). The *PET* during 2017 was of approximately 677 mm/year. The year 2018 is considered as a dry year with 870-875 mm of *VI* and slightly higher *PET* (702 mm/year). *PET* in 2017 is due to a slightly higher net radiation during the summer 2018 than the other two years. This might be explained by lower cloud cover and less precipitation events than in 2017. The precipitation in 2016 and *PET* are considered closer to normal conditions with *VI* of 1014 mm and *PET* of 672 mm. The *VI* values are similar between the three sites, except in 2016 where it was lower by 87 mm at STEL compared to SLZ station.

1.4.2 Site characteristics

At every site, a high K_s under approximately 40 cm depth was measured consistent with the dominant uniform sandy soil horizon to greater depth (Table 1.3). The textural analysis have been performed up to 90 cm depth at STEL and 120 cm at SLZ, thus the results of the last layer have been extended to the depth of the soil column (300 cm). None of the samples contained a clay fraction. STEL site shows the most drastic change in soil texture with depth. The first layer is rich in silt (13.2%) from 0 to 40 cm (compared to 7.4% for SLZ sites) with a measured K_s of 362 cm/day. Then it shifts to a silt fraction of 5.3% and a K_s of 1296 cm/day between 41 and 65 cm depth. This is coherent with field observations of a very dense and finer soil horizon between 20 and 50 cm approximately. At SLZ, the soil characteristics of the site A and B were considered differing only in their percentage of organic matter content and roots distribution, based on their proximity (15 m) and field observations. Therefore, the same results of textural analysis were used for both sites. An important difference can be seen in the measured K_s at 20 cm depth for both sites with a value of 1036 cm/day in the prairie and 240 cm/day in the forest. Therefore, they both retrieve similar conductivity at approximately 50 cm depth indicating they retrieved similar soil characteristics. It illustrates the importance of organic matter content and vegetation on water flow behavior at shallow depths. It is consistent with field observations during the drilling, where unconsolidated medium sand at SLZA and rich horizon in organic matter in the forest was observed, enhancing water holding capacity at shallow depth.

Therefore, the organic matter content was integrated in the soil textural distribution as a silt portion because soil moisture storage capacity is positively correlated with organic matter and silt fraction (Bot and Benites, 2005). The only soil textural distribution could not account for this difference between the two SLZ site. Wang et al. (2009b) found that increasing soil organic matter induced lower hydraulic conductivity in the sandy soils of the Nebraska Sand Hills, suggesting that soil carbon should be considered when estimating hydraulic conductivity. The high organic matter content observed in the forest is therefore considered to be an important component in soil characterization to represent the soil moisture behavior in the top layers of these permeable sediments. In the current study, the modification of the textural distribution to include organic matter contents resulted in initial parameters better representing the *in situ* hydraulic properties of the upper soil layer.

1.4.3 Soil moisture contents

1.4.3.1 Measured soil moisture contents

The volumetric water content (VWC) monitored are more variable in time within the first 30 cm at every site. This can be due to the higher organic matter content or silt fraction (Table 1.3), which enhance the soil water holding capacity, and to the tighter coupling between soil moisture and land surface processes at shallow depths (Guber et al., 2008; Martínez-Fernández and Ceballos, 2003). The VWC decrease with depth, are consistently lower, less variable in time and closer to the residual water content. This is coherent with the increasing sand fraction with depth (Table 1.3) promoting rapid percolation and lower water holding capacity.

The moisture behavior's relationship with silt and organic matter content is also illustrated in the dynamic of the data monitored at each site at shallow depth. The VWC measured by the first sensor at SLZA station (Figure 1.3) exhibit lower dynamic behavior with few small variations which are typical of coarse sediments characterized by low-holding capacity and favoring rapid drainage. It is contrasting with the VWC measured at SLZB, which is highly dynamic covering a large range of moisture contents (Figure 1.4). The maximum VWC measured in the forest at 10 cm depth is 0.47 with a mean of 0.16 while, in the prairie site A, a maximum of 0.26 and a mean of 0.12 have been monitored. A seasonal trend is also shown in Figure 1.4 with a decreasing mean water content during summer months. Those observed contrasted moisture dynamic support the integration of the organic matter in the silt proportion to account for field differences not reflected in the only soil textural distribution.

At STEL, there are two drought periods that were recorded in late summer by the first sensor in 2016 and 2018 (Figure 1.5). It might be explained by evaporation in the soil column due to a deficit in precipitation. But generally, the soil moisture content stays at mean high level of 0.29 to a maximum of 0.41 and the soil needs particularly dry conditions for many consecutive days to reach low water contents. Thus, more energy is necessary to evacuate the pore water in the denser and finer soil at STEL. Those characteristics allow a higher water holding capacity, comparable to SLZB site, but with less dynamic variations than the latter, which is more permeable. Therefore, the higher natural silt fraction in the first soil layer at STEL permits higher water retention and slow drainage. While the higher fraction of organic matter in the forest also enhance the water holding capacity similarly to STEL but allows the soil to drain more easily when mix with mostly medium sand.

Other studies have also shown that many factors influence soil hydraulic characteristics, including bulk density, organic matter, and pore size distribution (Schaap et al., 2001; Wang et al., 2009b). Therefore, the soil textural distribution coupled with field and laboratory experiments allow a proper characterization of the soil natural conditions consistent with field observations.

1.4.3.2 Simulated soil Moisture contents

One of the main issues associated with the simulation of *GR* comes from the correlation between hydraulic parameters leading to a non-unique calibrated model (Carrera et Neuman, 1986; McKenna et al., 2003). Reducing model dimensionality by setting some of the soil hydraulic parameters and thus removing them from the calibration process, has been shown to reduce the non-uniqueness problem (Jacques et al., 2002; Ritter et al., 2003). However, this approach may alter the ability of the model to accurately reproduce the observed data and estimate the soil capacity to retain or transmit water. It also remains difficult to choose the appropriate values of the soil hydraulic parameter. In many studies, the parameter θ_r is not calibrated (Thoma et al., 2014; Turkeltaub et al., 2015) because the objective function and the recharge estimates are found to be poorly sensitive to this parameter, which has been shown to have low identifiability in similar modeling experiments (Scharnagl et al., 2011; Šimůnek et al., 1998). In the current study, the VWC at the three sites varied mostly in the dry range, making it difficult to calibrate θ_s at a daily time step (rapid drainage and saturation state might not be properly represented) and the need to calibrate θ_r (the VWC vary mostly around this value almost representing a mean). Therefore, the parameter θ_s was not calibrated except for the first soil layer at STEL and SLZB where higher VWC were measured.

In the literature, the pore connectivity parameter l in the VGM model is often fixed at a value of 0.5 (Mualem, 1976), because it is considered unimportant or insensitive (Abbaspour et al., 2000; Wollschläger et al., 2009). This parameter apparently becomes sensitive at very low VWC (Vrugt et al., 2001), as suggested by Scharnagl et al. (2011), and was thus calibrated here.

The simulated daily soil moisture contents for the three sites (Figures 1.3, 1.4 and 1.5) represent relatively well the measured conditions at the four instrumented depths. For the purpose of brevity, only the calibrated VGM parameters for the above three sites are reported in Table 1.4 (see initial values and calibration bounds in supplementary Table 1.7 and 1.8). Based on the observed VWC from each site or on literature-based values for coarse materials, the calibration bounds to all parameters have been enforced.

The VWC observed and simulated at SLZA station for the calibration period show that the simulated values are overestimated in 2016 and underestimated in 2017 (Figure 1.3). This might be attributable to the evolving compaction of the sand after the installation of the sensors. The simulated VWC values at this site show more rapid variations than the measured values. The simulated soil column at this site is therefore very reactive to the atmospheric boundary conditions, which is typical of coarse sediments coupled with low organic matter content (Table 1.3). This might indicate the need to integrate an additional superficial fine soil layer in the first centimeter depth to dampen the infiltration rate and better represent natural conditions with vegetation. The VWC simulated at SLZB cover the large range of moisture contents monitored (Figure 1.4) and has reasonably reproduced the moisture dynamic and the seasonal trend in soil moisture content monitored. The simulated VWC from the calibrated model at STEL show a good fitting with the experimental data, although the magnitude of some short drought periods were not completely simulated in the summers 2016 and 2018 (Figure 1.5). It might be due to an underestimation of evaporation in the topsoil layers in the modeled soil column or misrepresentation of root density with depth. In general, the resulting soil moisture contents from the simulations corresponded well with the dynamic of the inputs of *VI* and were able to capture most of the observed soil moisture peaks and drainage processes.

For the goodness-of-fit assessment, the resulting values of RMSE, R^2, MAE are shown in Table 1.5 for the calibration period. The MAE values are below the accuracy of the soil moisture sensors (0.03) indicating that the simulated long-term soil water storage matched well with the observed ones. The ME is nearly 0 at every site demonstrating that there is no tendency for over-prediction or under-prediction. Singh et al. (2004) stated that RMSE values inferior to half the standard deviation of the experimental data may be considered appropriate for model evaluation. The RMSE is almost equal to half the standard deviation at SLZB (sd/2 = 0.030; RMSE = 0.032) showing an acceptable agreement with experimental data. The model at STEL exhibits the best fit with a RMSE of 0.014 compared to 0.054 for half the standard deviation while at SLZA both values are equal. The R^2 values show the same tendency with the best goodness-of-fit at STEL with a value of 0.98 followed by SLZA (R^2= 0.75) and SLZB (R^2=0.71) showing acceptable agreement between observed and simulated moisture content. The simulated VWC from the calibrated model at SLZB show the least satisfactory statistical agreement which might be caused by the increasing presence of natural heterogeneity in the forest ground more subject to create minor local discrepancies between the measurements and the simulation.

The calibration indicated that the Richards equation-based model can capture the major phenomenons revealed in the monitoring data obtained from the vadose zone of interest. Factors that might contribute to the deviation between observed and simulated VWC may come from a mismatch between the recorded precipitation or evapotranspiration rates, uncertainties in the observed soil moisture data and from the unaccounted-for heterogeneity of the soil layers like roots and macropores. It can potentially be attributed to the significant spatial variability of soil moisture and the degree to which the sensors are in contact with the soil material, especially in coarse soil. Nonetheless, the obtained statistical results from inverse modeling during the calibration period are within the general ranges of values found in previous studies (Assefa et Woodbury, 2013; Jiménez-Martínez et al., 2009; Min et al., 2015; Wang et al., 2016) indicating a good model performance.

1.4.4 Simulated recharge

1.4.4.1 Calibration period

The calibrated models were used to simulate the flow of water through the soil column and computed *GR* from 2016 to 2018 at each site. Inter-annual variability in *GR* existed at each site following the variation in annual *VI*. The simulated recharge range between 347 (SLZB 2018) and 735 mm/y (SLZA 2017) (Table 1.6). This large difference is due to the annual variation in precipitation and to the contrasted effect of vegetation and organic matter content on *GR*. STEL and SLZB sites resulted in similar recharge range with a maximum of 607 (STEL 2017) and 586 mm/y (SLZB 2017) and a minimum of 384 (STEL 2018) and 347 mm/y (SLZB 2018). Whereas SLZA produced a slightly higher range of recharge rate of greater magnitude with a maximum of 735 (2017) and a minimum of 487 mm/y (2018). Similar observations of inter-annual variability can also be made for *AET* which varied from 387 (SLZA 2018) to 619 mm/y (SLZB 2017). The maximum *AET* is obtained in 2017 for every site because the availability of water was not limiting.

The higher recharge rate and lower *AET* at SLZA are attributed to the coarser nature of the sediments in the root zone associated with small water-holding capacity. The precipitation arriving at the surface infiltrates almost instantaneously into the ground due to low organic matter content and drained through the root zone to recharge the underlying aquifer. This water flow behavior limits the uptake by plants. It is in concordance with field observations of unconsolidated and highly permeable sand at the surface and it explains the observed sparse vegetation at this location. The vegetation can thus be considered as an ecosystem adaptation to the natural site conditions like soil water retention, climate and water-table depth. The lowest *GR* was computed at SLZB, this is expected since the site is under forest cover and should consume more water by transpiration than prairie environments demonstrated by a systematic higher *AET*. The *GR* computed at STEL is significantly lower than at SLZA site, which is surprising because they represent similar land cover. Because of the finer soil texture at STEL in the first 40 cm depth, the water flow is slowed and the water-holding capacity is increased permitting higher *AET* rates compared to the other prairie site. The *AET* at STEL for the calibration period ranges from 479 to 604 mm/y while at SLZA it goes between 387 to 479 mm/y. This in fact, explains the similar *GR* estimated at STEL and SLZB exhibiting similar soil characteristics in the first centimeter depth (Table 1.3). The soil textural distribution in the root zone is thus an important factor controlling the flow processes in the vadose zone. Therefore, the *GR* computed at STEL in 2016 is significantly lower than at the two other sites. This might be explained by the precipitation values being 87 mm lower at this site in 2016 (Table 1.6). The latter result is not observed in the *GR* estimation made with the WTF method showing that it might come from input data in the model.

1.4.4.2 Comparison with the water-table fluctuation method

One of the main uncertainties in the *GR* estimates from the WTF method arises from the difficulties in estimating the specific yield. This parameter is treated as a storage term, that accounts for the instantaneous change in water storage upon a change in total head (Healy, 2010). Loheide et al. (2005) found that specific yields of coarse-grained sediments were generally similar to θ_s - θ_r. Thereby, the VGM parameters calibrated here have been used to calculate the storage term. A value of 0.33 and 0.34 has been found for SLZ and STEL site, respectively, and is comparable with literature values varying between 0.32 and 0.39 for a sandy soil according to Loheide et al. (2005). In addition, the WTF method can be hard to compute because it assumes that recharge occurs only when the water-table data exhibit well-defined rises. The coarse nature of the sediment permits steady groundwater recharge enabling the proper quantification of recharge rates by the attenuation of the water-level signal. For example, if the recharge rate to an aquifer is steady and equal to the drainage rates away from the aquifer, the groundwater level will not change, and the WTF estimate would result in no recharge event. In addition, not all fluctuations in groundwater levels indicate recharge events. Some artifacts can arise in the water-level time series from logger inaccuracy and the Lisse effect (Krul and Liefrinck, 1946) which affect the water level in unconfined aquifers by air entrapment between the water table and a wetting front.

The water levels at both sites exhibit a well-defined seasonal cyclic pattern of rapid rise in spring followed by a gradual decrease throughout the remainder of the year, although the water level at STEL is more subject to daily variations (see supplementary materials Figures 1.10 and 1.11). The borehole executed at STEL showed a silty soil layer with traces of sand and clay near the water table (4 to 6.5 m). The latter could explain the more dynamic behavior of the water-table levels at STEL site (average water-table depth of 5.5 and 6.8 m at SLZ and STEL respectively).

The *GR* results obtained by the WTF show the highest recharge rate at both sites in 2017 and the lowest in 2018 (Figure 1.6). This observed trend follows the variations in annual precipitation. Therefore, when both sites are compared, the *GR* is higher at STEL in 2016 and 2017 even if the precipitation at this site in 2016 were lower by 87 mm. While the *GR* at SLZ site is higher to the one computed at STEL in 2018. In addition, the WTF method gave higher *GR* rates than the one simulated by HYDRUS at STEL only in 2016 and 2017 as illustrate in Figure 1.6. In 2018, the water-table levels exhibit the least rises at both sites (supplementary Figures 1.10 and 1.11) because it is the driest year. The interpretation of those numerous small rises as recharge events in 2016-2017 might results in the summation of the uncertainty in S_y estimation or recharge events leading to the exaggeration of the estimated rates those years. The Lisse effect phenomenon is normally prevalent in fine-texture soils with shallow water table $<$ 1-1.3 m (Weeks, 2002), which is not the case herein. Therefore, the discontinuity between coarse and fine sediment around 4 m depth could be favorable for the air entrapment. In addition, the capillary rise could be important at this depth resulting in apparent recharge events from water arriving at a 4 m depth. This in fact, can cause the water-table level to rise with no recharge events and favor subsurface flow due to a deficit of infiltration in the less permeable horizon already close to saturation. In addition, there might be lateral groundwater inflows from further uphill causing potential artificial variations of the water table. Consequently, the water-table rises < 0.02 m at SLZ and < 0.04 m at STEL have been removed from the calculation to account for data logger inaccuracy and from interpretation of couple water table and precipitation time series. The water-table time series at SLZ show a less dynamic behavior leading to probably fewer misinterpretations of recharge events. It should also be noted that the SLZA site represents only an outcrop from a large forested zone (high *PET*) explaining the similar *GR* estimated by the WTF and the model in the forest because the groundwater level fluctuations are representative of a regional phenomenon. It could also be attributed to an underestimation of the drainage curve due to steady recharge process in coarser soil at SLZ. Also, the results from the WTF obtained at STEL gave similar *GR* estimation to the simulation at the other prairie site (SLZA) in 2016-2017, although slightly lower. The results from the WTF might indicate an overestimation on the control of fine-textured soil in the first centimeter depth at STEL or only a misinterpretation associated to the subjectivity of the water-table signal treatment discussed previously.

The model HYDRUS-1D gives insight into processes operating in the vadose zone at the local scale while the WTF method gives information at the regional scale and does not rely on meteorological data. Therefore, the absolute values of *GR* estimates with both methods should be interpreted with caution when local *GR* rates must be quantified. Despite the uncertainties associated with the S_y and the interpretation of recharge events, the WTF captured the whole inter-annual range of *GR* variability simulated by the model (Figure 1.6). The year 2017 is the wettest leading to the highest recharge rates and 2018 the driest, with the lowest recharge estimation at each site. This observed trend follows the variation in annual precipitation. Consequently, this approach represents a useful tool for estimating the possible range of *GR* independently of meteorological data or when only few data are available.

1.4.4.3 Long-term recharge estimation

The results show that for a mean rainfall of 994 and 968 mm/y at SLZ and STEL from 2004 to 2017, the estimated long-term mean recharge rates were 596, 457 and 448 mm/y at SLZA, SLZB and STEL, respectively. Those represent mean ratios of *GR/VI* corresponding to 59, 45 and 46% for SLZA, SLZB and STEL, respectively, ranging from 34 to 68% of annual *VI* following climatic variations. Based on model simulations from a spatial surface water budget, run from 1989 to 2009, Larocque et al. (2015) found that the areas of unconfined aquifers in Vaudreuil-Soulanges (9% of the region) receive a mean *GR* of 331 mm/y up to a mean maximum of 440 mm/y. This maximum mean falls in the same order of magnitude of the mean *GR* rate found by HYDRUS at SLZB and STEL suggesting high recharge rates computed by the vadose zone model. Therefore, the spatial model partitions the water budget in multiple components not accounted for in this study (runoff and subsurface flow) and considered negligible at local scale due to the coarse matrix (between 84-100% of sand) and flat topography. Those characteristics promote rapid infiltration and prevents runoff and subsurface flow during rain events at local scale. They estimated that the runoff and subsurface flow components were accounting for 56% of *VI* corresponding to a mean of 540 mm/y for the whole region. Those water budget components generate estimates that fall within the range of *GR* and ratios of *GR/VI* computed by HYDRUS-1D at the IRRES stations. Concerning the evapotranspiration results, Larocque et al. (2015) found that the mean annual *AET* represents 39% of *VI*. Another bucket model used on the Rivière à la Raquette watershed located in the Vaudreuil-Soulanges estimated that *AET* could account for 46% of *VI*. Those ratios are lower than the findings in this study but still in the same range of magnitude with mean ratios of *AET/VI* of 43, 57 and 56% for SLZA, SLZB and STEL, respectively. The discrepancies between the results can arise from different spatial scales considered within each model. The HYDRUS-1D model produces a highly local estimate and the spatial water budget model computes *GR* estimations on a 250 m grid without considering explicitly vegetation and soil characteristics. Barbecot et al. (2018) estimated *GR* at STEL from 2010 to 2013 with a hydro-isotopic water budget. They found a *GR* of 200-372 mm/y occurring only for snow melt with an *AET* of 608-517 mm/y. At STEL, for the same period, a mean *GR* and *AET* of 400 and 542 mm/y were calculated by HYDRUS. The results from the hydro-isotopic water budget and from the model used herein are in the same order of magnitude and in good agreement.

1.4.5 Factors controlling recharge

1.4.5.1 Seasonality of recharge processes

Over the entire simulated period, the monthly *GR* rates show strong annual and seasonal variations (Figure 1.7). The main recharge peaks occur during the spring, with a maximum value in April, and then declined rapidly for the summer period when evapotranspiration starts to be significant. The magnitude of the estimated recharge in March and April fluctuates due to variations in starting snow melt period and the accumulated snow cover during the winter period. Those observations indicate the significant role of the snowpack on the *GR* pattern. Another recharge period is observed during fall, but to a lesser degree with maximal possible rates from October and December depending on the year and site. The same observations were made by Larocque et al. (2015) who found that *GR* from March to May represents 38% of annual recharge and in fall (October to December), *GR* represents 44% of annual recharge from the spatial surface water budget. At the IRRES station, the spring *GR* represents a mean of 38% for SLZA and 45% for SLZB and STEL of annual recharge, while in fall it represents 29% at SLZA and 30% at SLZB and STEL. Therefore, it should be noted that those ratios are highly variable between years.

As seen in Figure 1.7, the inter-annual variability of monthly *GR* is the largest during spring and fall when *PET* is negligible and snow cover conditions can be highly contrasted from year to year. Fall evapotranspiration and the timing of spring snow melt apparently control the timing of the preferential recharge periods, while precipitation controls mainly the magnitude and inter-annual variability in *GR* rates. This seasonality in *GR* processes might be an important factor to consider in southern Quebec where precipitation is expected to increase under climate change (Ouranos, 2015). It is possible that increases in precipitation will be dampened by increased *PET* resulting from higher temperatures, especially if higher precipitation occurs during the summer period. On the opposite, if more precipitation occurs during the spring when *AET* is equal to *PET* and groundwater levels are high, climate change could lead to more runoff and eventually more floods. Milder winter might also be an important issue to consider in a climate change context, because it could influence the actual seasonality of GR by producing episodic recharge events during the winter period and reduce spring recharge volume.

1.4.5.2 Distribution of precipitation

The highest annual recharge occurred in 2005 for STEL and SLZB (601 and 622 mm/y) while at SLZA it occurs in 2006 (775 mm/y). Considering only SLZB as an example, the three years with the highest annual *VI* are 2006, 2017 and 2005 with, respectively, 1215, 1196 and 1091 mm, while the recharge rates for those same years, respectively, are 594, 585 and 622 mm. If precipitation is considered to be the main component controlling recharge volume in coarse soils, the highest annual *GR* should occur in 2006 (this is the case at SLZA). The difference appears in the distribution of *VI* all along the year. As shown in Figure 1.8, 2005 is characterized by an important recharge event in April and October concurrently to months with high *VI* values. In 2006, the precipitation is distributed more equally between months with a medium intensity recharge event from February to May and in the fall resulting from an early snow melt.

In 2017, there is again an important recharge event in April but also in March and May due to important precipitation during these periods mixed with higher than average snow accumulation and early snow melt. The *GR* period in fall 2017 is of lesser magnitude compared to 2005 and 2006 due to smaller precipitation during this period. In summary, higher water inflows during the spring and fall periods that are not compensated by higher evapotranspiration, induce excess water flowing rapidly through the root zone, resulting in higher recharge rates. Because plant water uptake at SLZA is limited by coarser sediments in the first soil layer, the highest recharge estimation corresponds well with the highest annual precipitation. Apart from the effects of meteorological conditions, soil properties at the study sites controlled the soil moisture and thus the *AET* and subsequently the *GR*.

1.4.5.3 Antecedent Moisture content

The minimum mean value of recharge is obtained in July, August and September at every site (Figure 1.7). Although the *PET* starts to be higher than the mean monthly *VI* in May and September. They should thereby have similar recharge rates, while the variability in monthly recharge rates is significantly higher in May at every sites. This might be attributed to the antecedent moisture content of the preceding month. The recharge rate in late spring and in the beginning of the summer is preceded by the two wettest months (March and April), while in September it is preceded by the two driest months. The recharge starts to increase mostly in October when the potential values of *PET* become significantly lower than *VI*. The annual *GR* were plotted against the *VI* values of the preceding year and no significant correlation was found (not shown here). The recharge fluxes are thus mainly influenced by relatively recent precipitation patterns and antecedent moisture content (1-2 months).

1.4.6 Effect of meteorological datasets on groundwater recharge

The three different runs with varying configurations of the ANUSPLIN and NARR datasets as input data were performed to assess the impact of their utilization on *GR* estimation. First, the run with the NARR scenario results in significant underestimation of *GR* in every year (Figure 1.9). This result is consistent with the fact that average annual precipitation from NARR is considerably lower than the observed values at STEL. There is a difference of 38% between the *VI* calculated with ANUSPLIN and NARR datasets. Secondly, the *GR* computed with the ANUSPLIN scenario is lower than the one performs with the combined scenario even if they have the same *VI* as input. It is owed to the calculation of *PET* in the ANUSPLIN scenario, computed with the temperature data as a proxy for radiation terms. The use of NARR dataset enables the calculation of net radiation without approximating it from temperature data. Sentelhas et al. (2010) found by comparing multiple *PET* formulas with different degrees of missing data that solar radiation had the most impact on *PET* calculation. Even though the radiation data from NARR exhibit an overestimation during summer compared to the measurements made at the STEL station, they gave lower *PET* values (closer to the ones calculated with STEL measurements) resulting in higher *GR* rates for the combined scenario. As a comparison purpose with other published works, Langlois et al. (2009) drove three snow models with NARR data in southern Quebec during three winters between 2004 and 2008. All the models gave accurate results compared to the simulations driven by data from a ground-base station or measurements of snow water equivalent. They demonstrated that the regional reanalysis can be used in snow models to predict snow water equivalent in Quebec. Also, Choi et al. (2009) demonstrated the applicability of NARR temperature and precipitation data for modeling hydrological processes in northern Manitoba. Therefore, for areas without direct measurements of radiation or *AET*, the NARR dataset might provide additional valuable information for the calculation of *PET* and the underestimation of precipitation might differ from location and period considered for study.

1.5 Conclusion

The results obtained in this study provide reasonable estimations of the renewal rate of groundwater in the preferential recharge areas of the Vaudreuil-Soulanges region. In the study zone, groundwater is increasingly used as a source of fresh water. The impacts of soil and climatic conditions on *GR* were examined using a network of soil moisture monitoring network in southern Quebec for inverse modeling with HYDRUS-1D. This approach is easy and cheap to implement and was found to be suitable and original for the Canadian context. The overall soil moisture contents simulated were able to capture the major phenomenons revealed in the monitoring data and corresponded well with the dynamic of the input *VI*. The soil textural distribution could not systematically account for soil heterogeneity in the forest ground. The model's inability to fully describe the experimental data stemmed from the gap between model representation and disincorporation of more complex processes and structures present in natural context. The model assumes soil column with homogenous sediments and no heterogeneity while, in fact, it may be affected by those causative factors. Nonetheless, the obtained statistical results from inverse modeling are within the general range of values found in previous studies indicating a good model performance.

The vadose zone model permitted the quantification of the water balance components in the Vaudreuil-Soulanges region. The *GR* simulation by the model and the WTF method were able to capture the whole inter-annual range of *GR* variability following the variations in annual precipitation. The main recharge peaks occur during the spring and fall, with a maximum value in April. It can be concluded that the evapotranspiration and snow cover control the timing of the recharge periods, while the precipitation controls the magnitude and inter-annual variability in *GR* rates. This seasonality in *GR* processes might be an important factor to consider in a climate change perspective, where the precipitation should increase in Quebec.

The results showed the importance of soil properties in controlling soil moisture levels and thus relevant hydrogeological processes. Under similar conditions of precipitation and *PET*, the ratios of *GR/VI* were considerably larger for the sandy prairie site at SLZA, while the other model in a prairie land cover (STEL) simulated *GR* closer the one obtained in the forest (SLZB). This is owed to their similar soil characteristics through the root zone.

The lack of complete and reliable meteorological datasets is often a limiting factor in Canadian studies. The accuracy of such datasets is not systematically questioned prior to using them for hydrogeological modeling and were found to have a major control on *GR* estimation. In this study, the differences between two publicly available meteorological datasets have been quantify. The main discrepancy arises in the NARR precipitation data exhibiting a substantial underestimation. It leads to underestimation of *GR* when solely NARR data were used as input values to the model. Nonetheless, with the same precipitation as input to the model the ANUSPLIN and combined scenarios gave different *GR* rates owed to the temperature data used as a proxy for the calculation of radiation terms. For areas without direct measurements of radiation or *AET*, the NARR dataset might provide additional valuable information for the calculation of *PET* and the underestimation of precipitation might differ from location or period considered for study. The interpretation of the comparison results of NARR and ANUSPLIN data with the weather station should be conducted with caution. In other situations, the quality of the NARR dataset could be better than suggested herein. Indeed, other studies performed in Canada demonstrating the overall reliability of NARR dataset for hydrogeological modeling have been mentioned earlier.

This study offers guidance to groundwater modelling practitioners by highlighting the main controls on recharge and the processes occurring in the vadose zone in a Canadian context. The unsaturated zone is often omitted in many studies but was found to be of great interest for understanding important processes herein. As in every model, this vadose zone model could not fully consider every process and mechanism occurring in the natural environment, but the procedure could still be suitable for model parameterization in other geological or climatic context. Despite the important uncertainties associated with each *GR* estimation methods, every new analysis brings important insights for the scientific community and for groundwater authorities in developing more efficient strategies to ensure the sustainable management of the groundwater resource.

1.6 Acknowledgements

This work was funded by the Natural Sciences and Engineering Research Council of Canada (NSERC) discovery grant to Florent Barbecot and a scholarship from MITACS. The installation of the IRRES network was funded by the Canadian Foundation for Innovation (CFI). The authors would like to thank the private landowners and natural parc for making their property available for this study. The authors thank Sylvain Gagné, Marina Tcaci and François Hardy for technical support.

1.7 Tables

Table 1.1 Recharge monitoring site characteristics.

Station	Land cover	Depth of VWC sensors	Time period
SLZA	Grassland	10, 20, 50 and 100 cm	2015-08 to 2018-12
SLZB	Jack pine forest	10, 20, 50 and 100 cm	2016-10 to 2018-12
STEL	Prairie Grassland	25, 50, 75 and 100 cm	2015-12 to 2018-12

Table 1.2 Description of daily meteorological variables used for comparison, where T stand for air temperature and P for precipitation.

Dataset name	Source	Type	Variable	Time period	Coverage
STEL	IRRES station at Saint-Telesphore site	Surface station observation	T, P, longwave and shortwave radiation, wind speed	2016 to present	local
ANUSPLIN	Natural Resources Canada (NRCan)	Interpolated	Tmin, Tmax, P	1950 to 2017	10 km grid across Canada
NARR	NOAA's National Center for Atmospheric Prediction (NCEP)	Reanalysis	Tmin, Tmax, P, longwave and shortwave radiation, wind speed, albedo	1979 to present	32 km grid across North America

Table 1.3 Soil layer characterization at the three study sites from field and laboratory analysis.

IRRES site	Soil layer depth (cm)	Sand (%)	Silt (%)	Organic matter (%)	K_s (cm/day)
SLZA	0-15	92.7	7.4	2.7	
	16-30	92.7	7.4	0	1036
	31-70	96.7	3.3	0	950
	71-300	100	0	0	
SLZB	0-15	92.7	7.4	6.9	
	16-30	92.7	7.4	5.4	241
	31-60	96.7	3.3	3	820
	60-300	100	0	0	
STEL	0-40	86.8	13.2	2.5	362
	41-65	94.7	5.3	0	1296
	66-80	94.7	5.3	0	1900
	81-300	98.8	1.2	0	

Table 1.4 Optimized van Genuchten-Mualem (VGM) parameters for the three IRRES sites.

IRRES site	Soil layer depth (cm)	θ_r (-)	θ_s (-)	α (1/cm)	n (-)	K_s (cm/day)	l (-)
SLZA	0-15	0.073	0.390	0.075	1.94	161	0.049
	16-30	0.032	0.387	0.036	3.54	1714	0.068
	31-70	0.076	0.382	0.033	4.5	1782	0.418
	71-300	0.020	0.376	0.023	3.82	1350	0.311
SLZB	0-15	0.040	0.442	0.020	3.32	160	0.024
	16-30	0.022	0.393	0.048	2.55	400	0.474
	31-60	0.004	0.386	0.035	2.75	508	0.523
	60-300	0.058	0.376	0.034	4.39	1154	0.502
STEL	0-40	0.011	0.378	0.041	1.12	143	1
	41-65	0.037	0.385	0.029	4.15	2498	0.001
	66-80	0.042	0.385	0.034	4.38	2373	0.010
	81-300	0.043	0.379	0.038	4.47	2497	0.857

Table 1.5 Goodness-of-fit measures for simulated and observed soil moisture values during the calibration period.

	SLZA	SLZB	STEL
R^2	0.75	0.71	0.98
ME	0.0009	0.0028	-0.00004
MAE	0.012	0.021	0.008
RMSE	0.018	0.032	0.014

Table 1.6 Simulated water-budget components of the model at the three study sites for the calibration period (mm/y). *GR* stands for groundwater recharge, *VI* for vertical inflows, *PET* potential evapotranspiration and *AET* actual evapotranspiration.

IRRES site	Water-budget component	2016	2017	2018
SLZA	*GR*	626	735	487
	VI	1014	1196	875
	PET	672	676	702
	AET	398	479	387
SLZB	*GR*	543	586	347
	VI	1014	1196	875
	PET	672	676	702
	AET	500	619	514
STEL	*GR*	456	607	384
	VI	926	1187	870
	PET	678	678	701
	AET	479	604	484

1.8 Figures

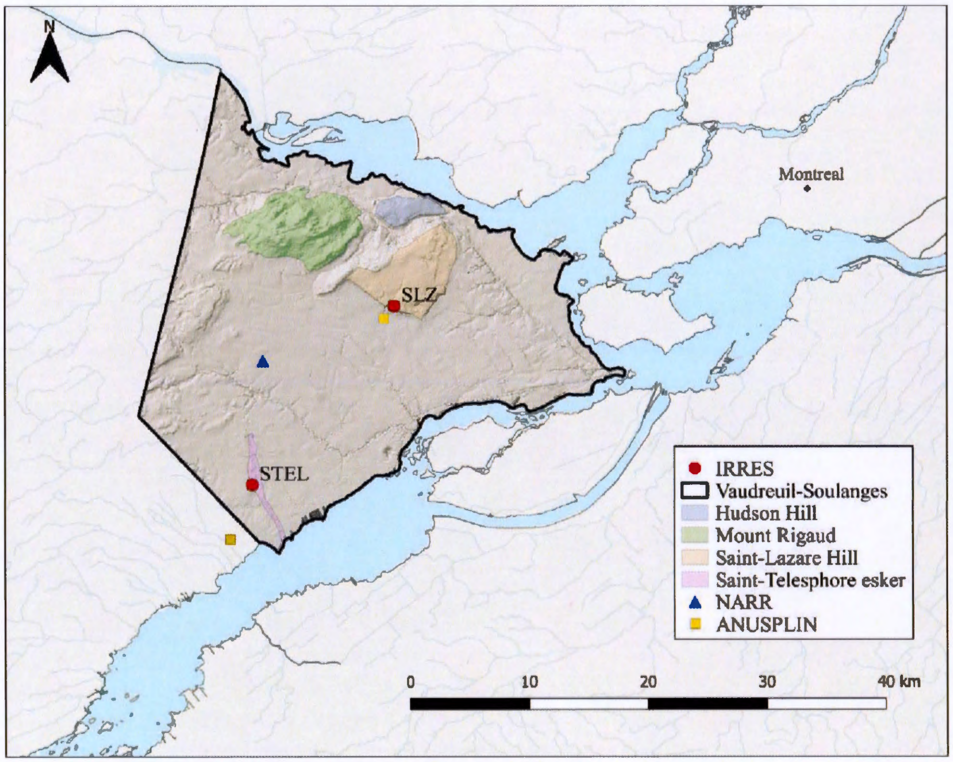

Figure 1.1 Location of the study sites in Vaudreuil-Soulanges region from the IRRES network and the position of the extracted meteorological datasets.

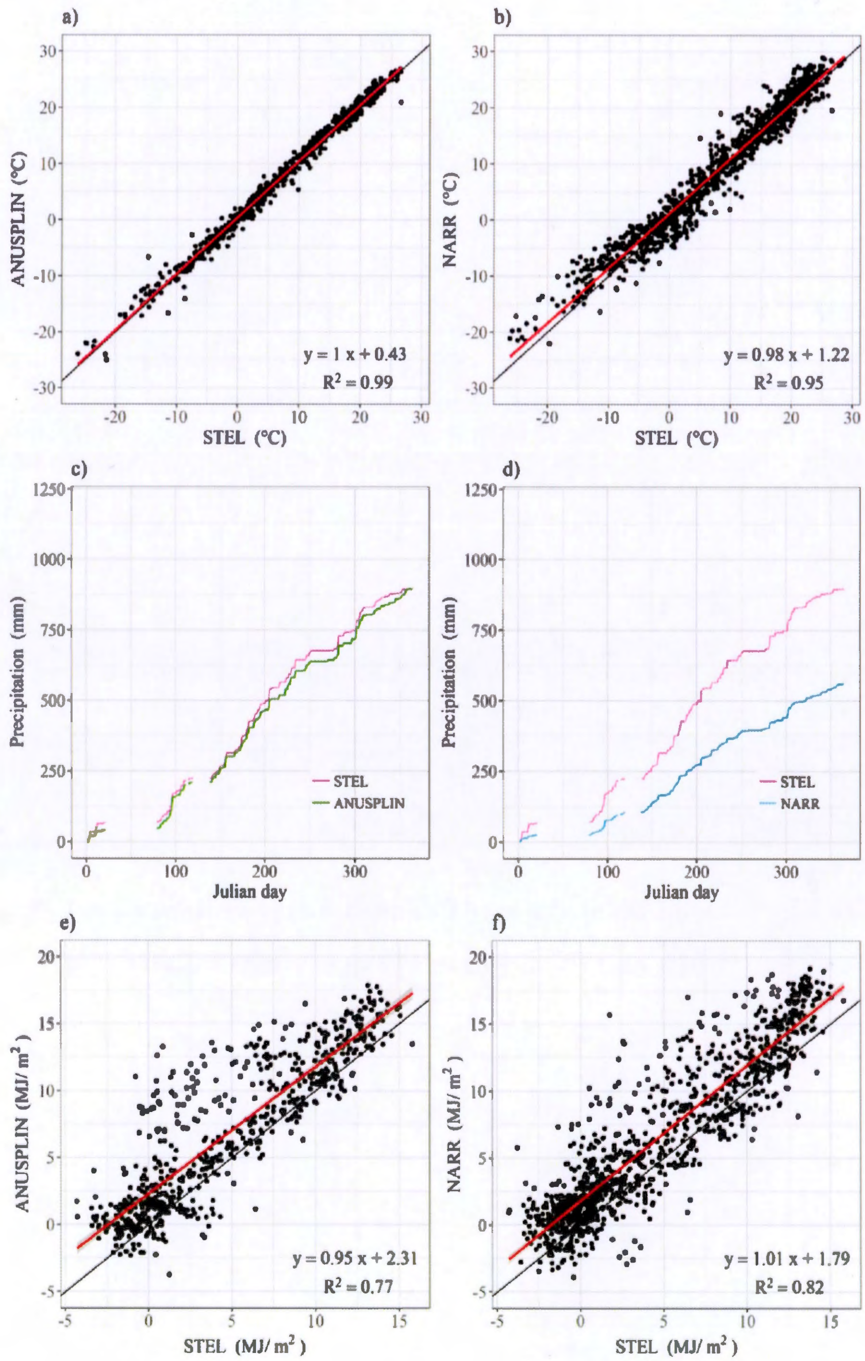
a)
b)
ANUSPLIN (°C)
NARR (°C)
STEL (°C)
y = 1 x + 0.43
R² = 0.99
y = 0.98 x + 1.22
R² = 0.95
c)
d)
Precipitation (mm)
Julian day
STEL
ANUSPLIN
NARR
e)
f)
ANUSPLIN (MJ/ m²)
NARR (MJ/ m²)
STEL (MJ/ m²)
y = 0.95 x + 2.31
R² = 0.77
y = 1.01 x + 1.79
R² = 0.82

Figure 1.2 Comparison of meteorological variables from the Australian National University Spline (ANUSPLIN) dataset in left column and North American Regional Reanalysis (NARR) dataset in the right column against data monitored at STEL site: (a) and (b) show linear regression of mean daily temperature,(c) and (d) cumulative precipitation in 2017, (e) and (f) linear regression of the net radiation taken from NARR and calculated from temperature for ANUSPLIN dataset.

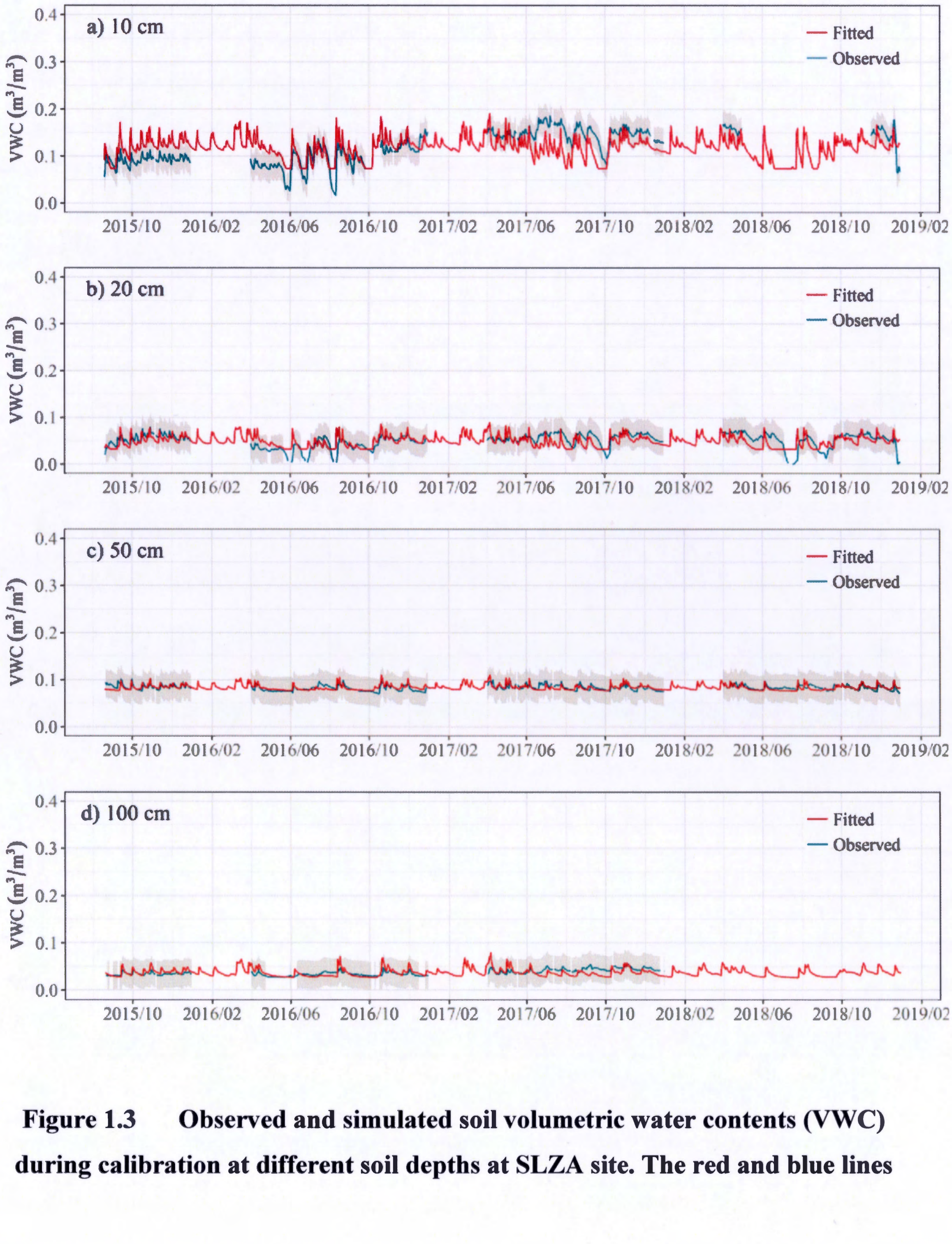

Figure 1.3 Observed and simulated soil volumetric water contents (VWC) during calibration at different soil depths at SLZA site. The red and blue lines

represent fitted and observed daily mean soil moisture content values and the gray areas indicate the accuracy of the sensor from generic calibration.

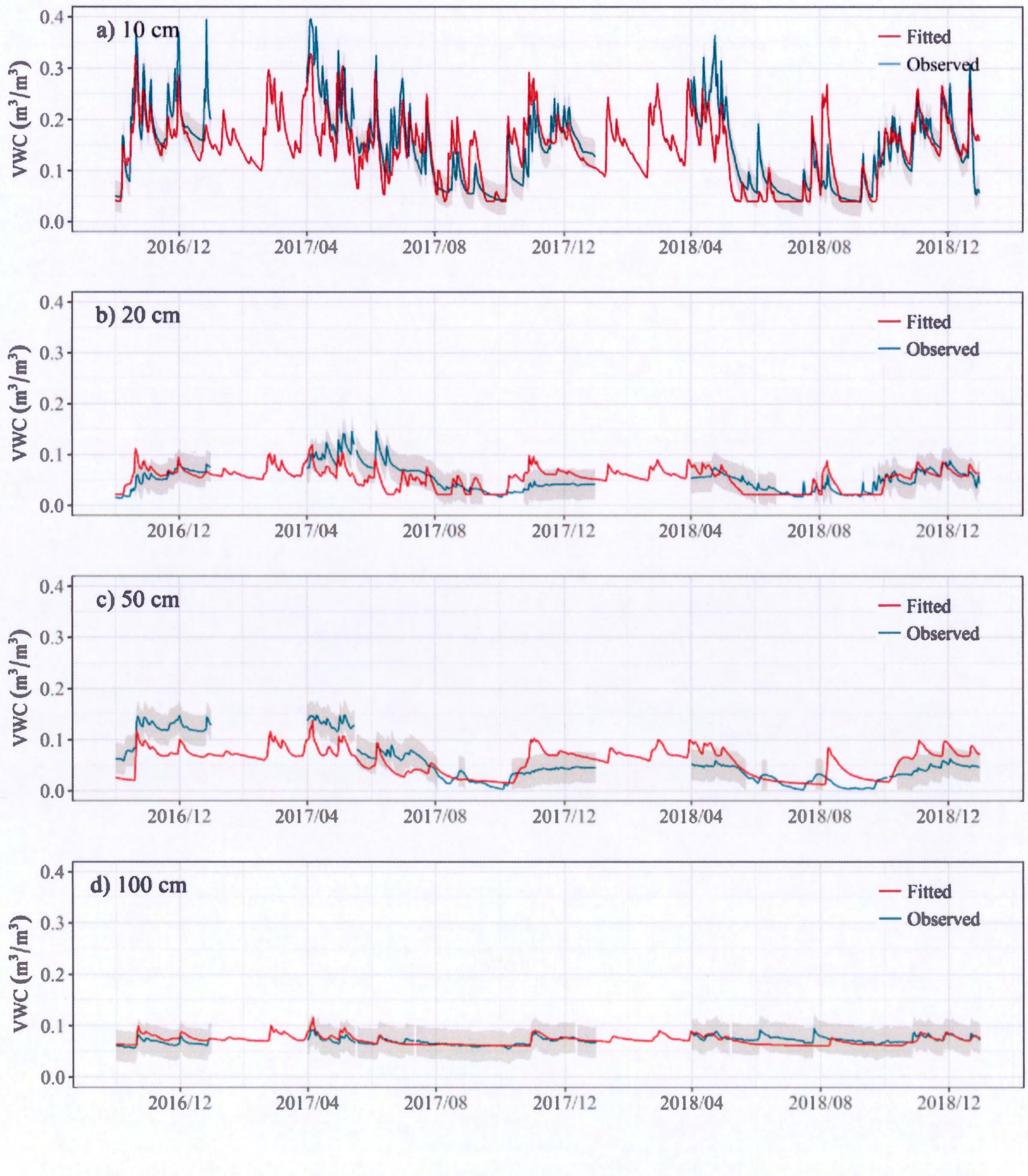

Figure 1.4 Observed and simulated soil volumetric water contents (VWC) during calibration at different soil depths at SLZB site. The red and blue lines

represent fitted and observed daily mean soil moisture content values and the gray areas indicate the accuracy of the sensor from generic calibration.

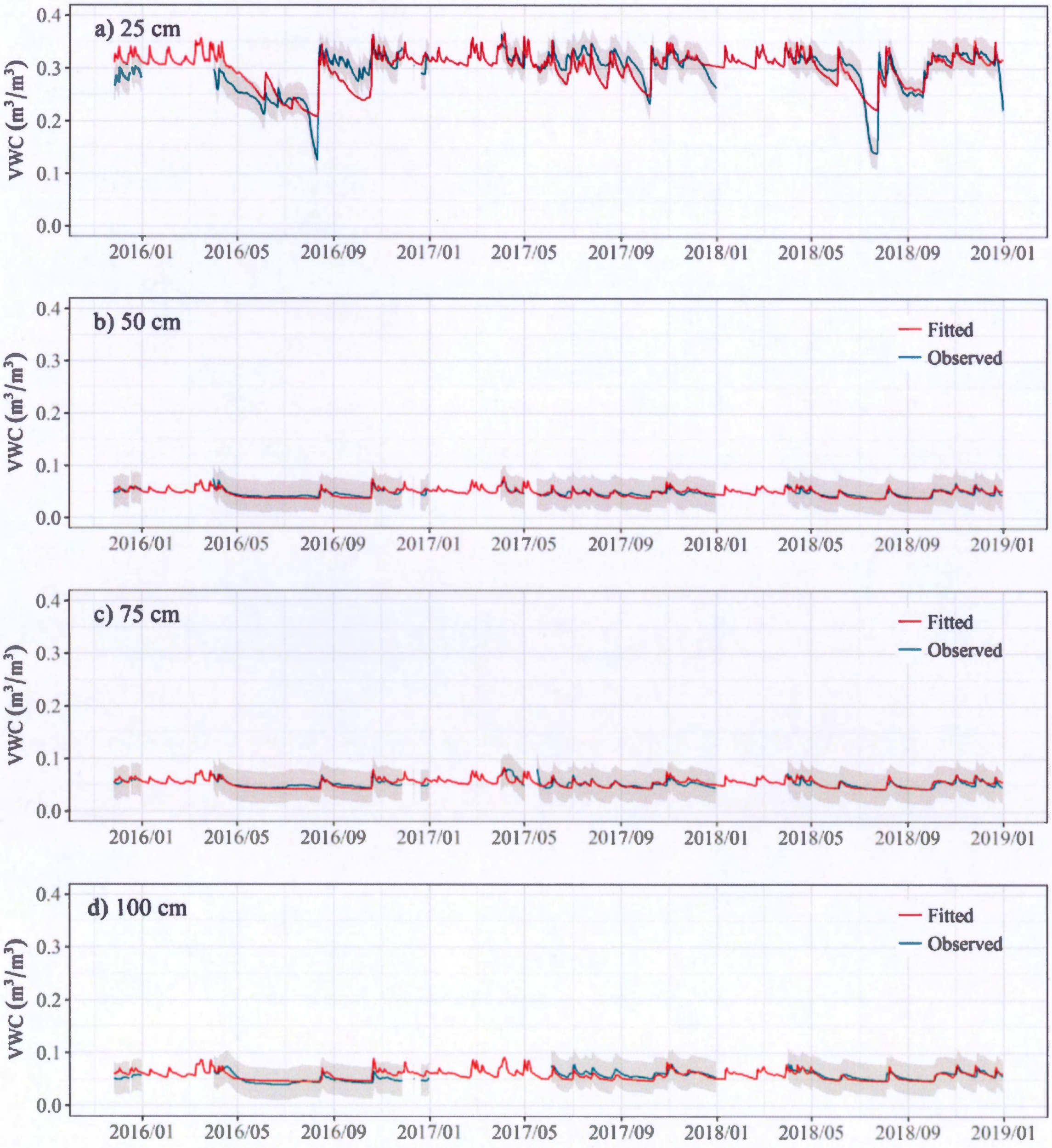

Figure 1.5 Observed and simulated soil volumetric water contents (VWC) during calibration at different soil depths at STEL site. The red and blue lines

represent fitted and observed daily mean soil moisture content values and the gray areas indicate the accuracy of the sensor from generic calibration.

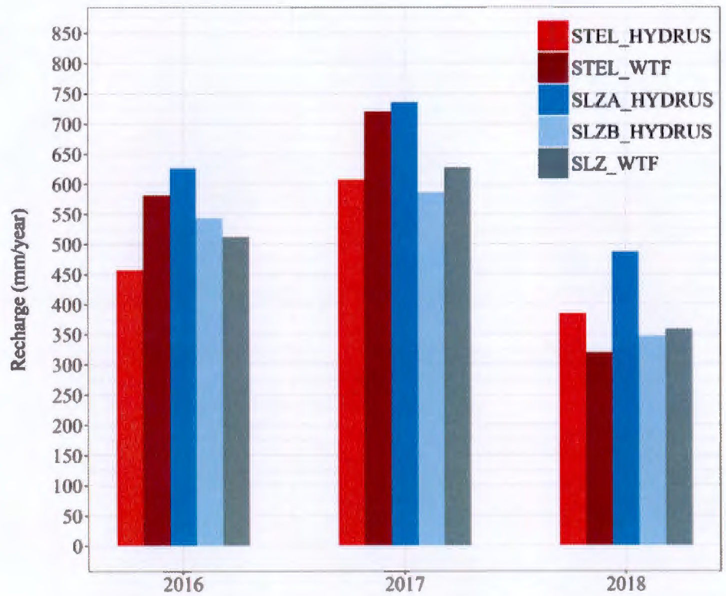

Figure 1.6 Groundwater recharge estimation results from HYDRUS-1D and the water-table fluctuation (WTF) method for the calibration period at the three study sites.

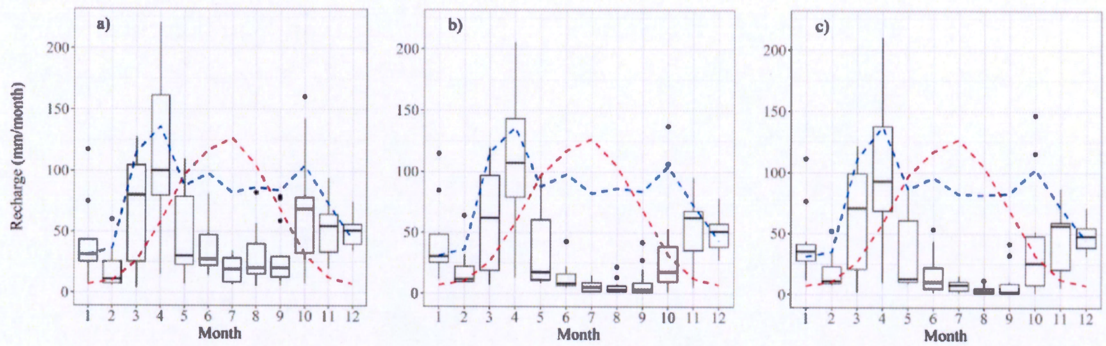

Figure 1.7 Monthly median, 25th and 75th percentile results for HYDRUS-simulated groundwater recharge estimates from 2004 to 2017 at the three study sites: (a) SLZA, (b) SLZB, (c) STEL. The blue and the red lines represent monthly mean vertical inflows (*VI*) and potential evapotranspiration (*PET)* respectively for the simulation period. The points represent outlier values.

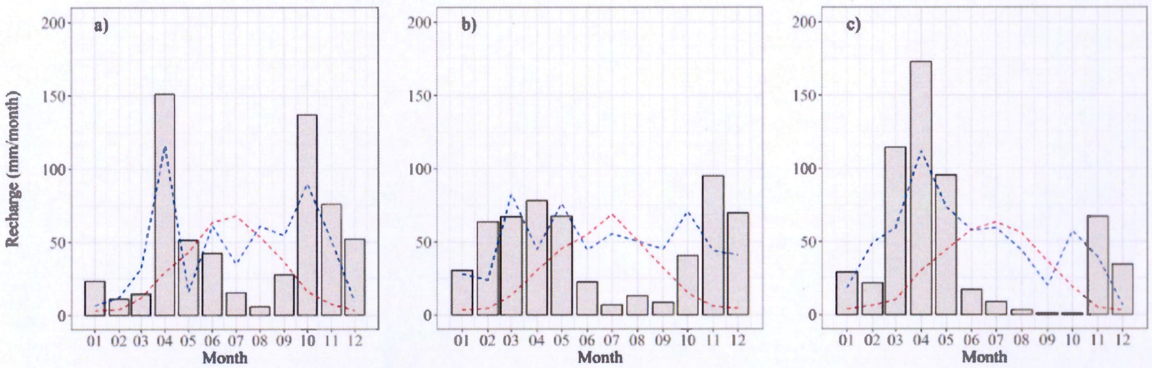

Figure 1.8 Monthly groundwater recharge for the study site SLZB in (a) 2005, (b) 2006, (c) 2017. The blue and the red lines represent the monthly mean vertical inflows (*VI*) and potential evapotranspiration (*PET*) respectively.

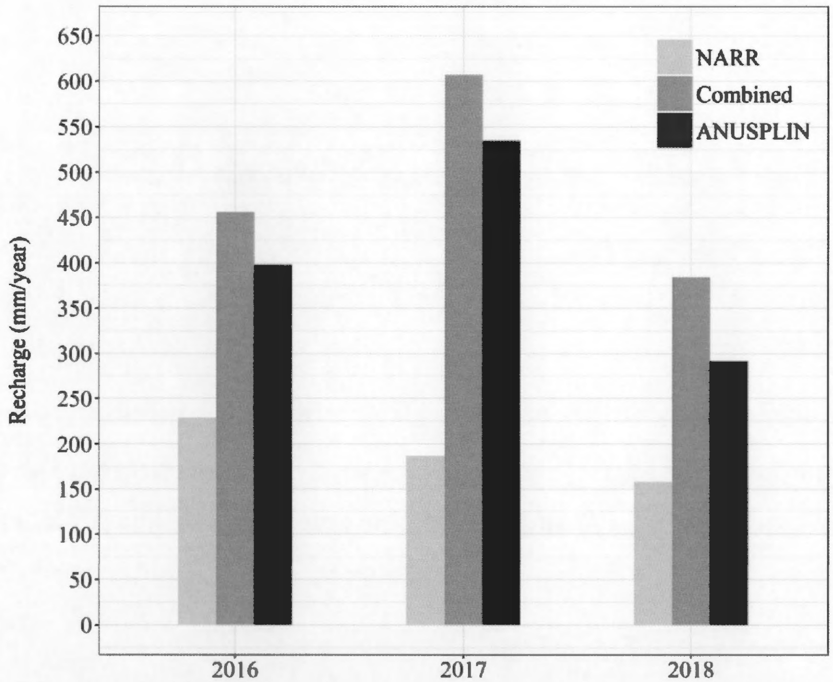

Figure 1.9 HYDRUS-simulated groundwater recharge for 2016, 2017 and 2018 at STEL site with the three different meteorological scenarios.

1.9 Supplementary materials

Table 1.7 Initial van Genuchten-Mualem (VGM) parameters as input values to the vadose zone model.

IRRES site	Depth (cm)	θr (-)	θs (-)	α (1/cm)	n (-)	K_s (cm/day)
SLZA	0-15	0.040	0.39	0.043	2.74	375
	16-30	0.043	0.39	0.041	3.16	1036
	31-70	0.048	0.38	0.037	3.84	950
	71-300	0.051	0.38	0.034	4.42	950
SLZB	0-15	0.035	0.39	0.048	2.22	216
	16-30	0.037	0.39	0.046	2.39	241
	31-60	0.044	0.39	0.040	3.26	820
	60-300	0.051	0.38	0.034	4.42	950
STEL	0-40	0.034	0.40	0.049	2.08	362
	41-65	0.046	0.38	0.039	3.49	1296
	66-80	0.046	0.38	0.039	3.49	1296
	81-300	0.050	0.38	0.035	4.21	1900

Table 1.8 Calibration bounds for the van Genuchten-Mualem (VGM) parameters used in model calibration.

IRRES site	Layer	θr (-)	θs (-)	α (1/cm)	n (-)	K_s (cm/day)	l (-)
SLZA	1	0.001-0.1		0.01-0.40	1.1-3.0	100-700	-1 to 1
	2	0.001-0.1		0.01-0.40	1.1-4.5	700-2000	-1 to 1
	3	0.001-0.1		0.01-0.50	2.0-4.5	700-2000	-1 to 1
	4	0.001-0.1		0.01-0.50	2.0-4.5	700-2000	-1 to 1
SLZB	1	0.001-0.05	0.39-0.60	0.01-0.40	1.1-3.5	100-500	-1 to 1
	2	0.001-0.05		0.01-0.40	1.1-3.5	100-1000	-1 to 1
	3	0.001-0.05		0.01-0.40	1.5-4.5	500-1500	-1 to 1
	4	0.001-0.1		0.01-0.40	2.0-4.5	500-2000	-1 to 1
STEL	1	0.01-0.20	0.35-0.50	0.005-0.5	1.1-3.5	100-700	-1 to 1
	2	0.001-0.05		0.01-0.40	3.0-4.5	700-2500	-1 to 1
	3	0.001-0.05		0.01-0.40	3.0-4.5	700-2500	-1 to 1
	4	0.001-0.05		0.01-0.40	3.0-4.5	700-2500	-1 to 1

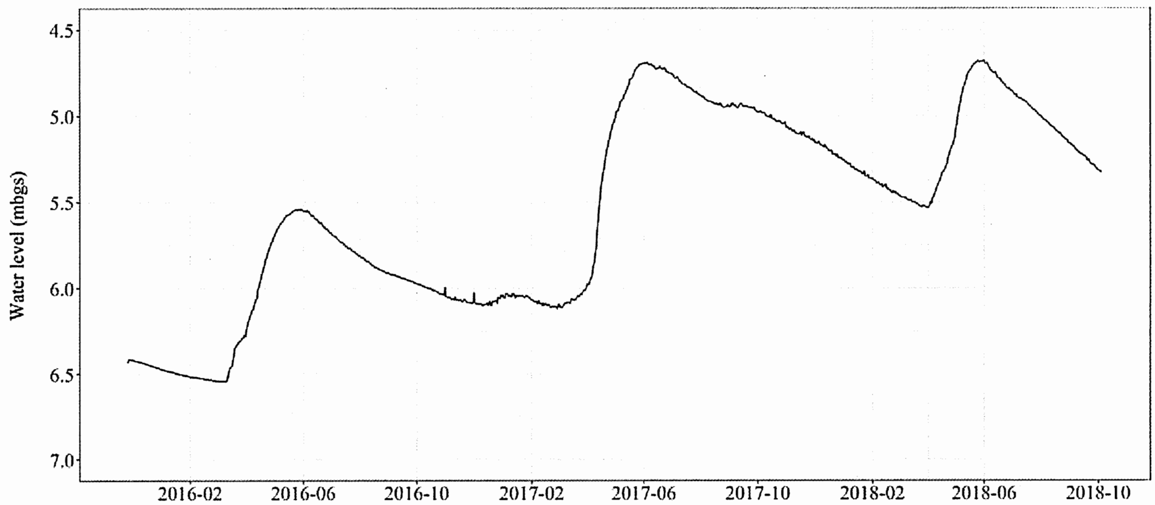

Figure 1.10 Measured groundwater levels (depth below the ground surface) at the SLZ site from 2016 to 2018.

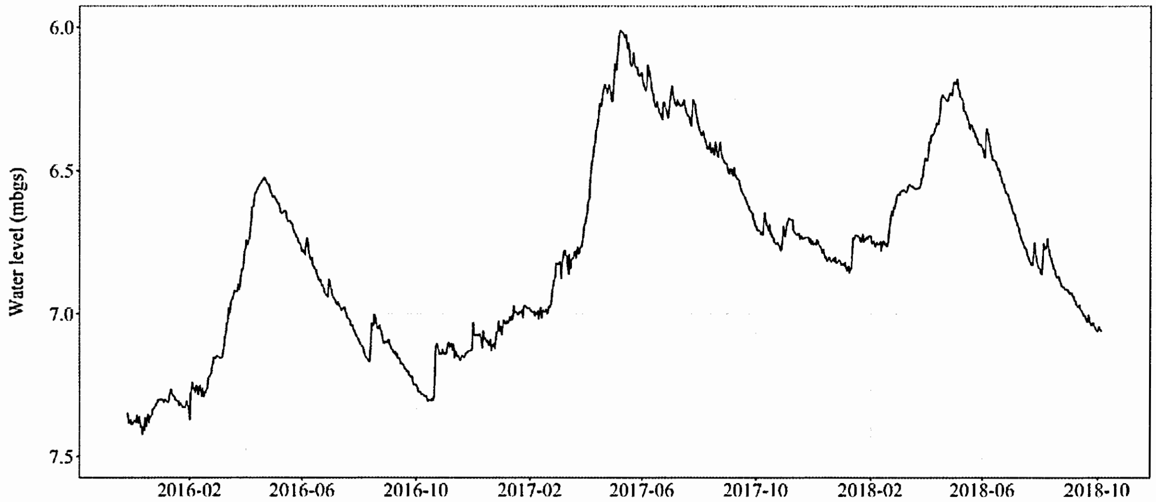

Figure 1.11 Measured groundwater levels (depth below the ground surface) at the STEL site from 2016 to 2018.

CONCLUSION

Les résultats obtenus dans cette étude fournissent des estimations raisonnables du taux de renouvellement de l'eau souterraine dans les zones de recharge préférentielle de la région de Vaudreuil-Soulanges. Dans la région d'étude, l'utilisation de l'eau souterraine comme source d'eau potable est en constante augmentation. L'influence des caractéristiques du sol et des conditions climatiques sur la recharge a été investiguée à l'aide du réseau de stations de suivi de la teneur en eau du sol au sud de la province de Québec par modélisation inverse à l'aide d'HYDRUS-1D. Cette approche est simple à mettre en œuvre en plus d'être adéquate et originale pour le contexte québécois. Les teneurs en eau simulées par le modèle ont, de manière générale, réussi à reproduire les phénomènes importants et les tendances représentées par les données enregistrées à chacun des sites. Les caractéristiques granulométriques des échantillons de sol n'ont pu systématiquement considérer convenablement les hétérogénéités du sol particulièrement en zone forestière. Les écarts entre les valeurs mesurées et simulées s'expliquent par les simplifications requises dans le modèle pour représenter les structures complexes, comme les hétérogénéités du sol, présents dans le milieu naturel. Le modèle représente une colonne de sol aux sédiments homogènes dépourvue d'hétérogénéités soumises à un écoulement vertical, quand en réalité, elle peut être affectée par une variété de facteurs naturels créant des discontinuités. Néanmoins, les résultats statistiques obtenus suite à l'inversion se retrouvent dans les intervalles de valeurs généralement obtenus dans le cadre d'études précédentes. Ceci démonte l'applicabilité de la procédure utilisée pour la paramétrisation de modèle dans la région d'étude.

Le modèle calibré de la zone non saturée a permis de quantifier les composantes du bilan hydrique dans la région de Vaudreuil-Soulanges. La simulation de la *GR* par le modèle et la méthode de la WTF ont pu capturer l'étendue des variations interannuelles de la recharge suivant principalement les variabilités des précipitations. Les pics de recharge principaux se produisent durant le printemps et l'automne, avec une valeur maximale en avril. Les résultats montrent que l'évapotranspiration et le couvert de neige contrôlent la temporalité des périodes de recharge, tandis que les précipitations contrôlent la magnitude et la variabilité interannuelle des taux de recharge. Cette saisonnalité des processus de recharge pourrait s'avérer être un facteur important à considérer dans une perspective de changements climatiques, ou les précipitations devraient augmenter dans la province de Québec.

Les résultats montrent l'importance des propriétés du sol dans le contrôle des niveaux de teneur en eau et ainsi son influence sur les processus hydrogéologiques. Sous des conditions similaires de précipitations et de *PET*, le ratio de *GR/VI* est considérablement plus grand pour les sites sableux situés en prairie à SLZA, tandis que le second modèle également situé en milieu de prairie (STEL) montre des résultats de *GR* similaires à ceux obtenus dans la forêt (SLZB). Ceci est dû aux caractéristiques du sol dans la zone racinaire qui sont similaires aux deux stations.

Le manque de données météorologiques fiables et complètes constitue souvent un facteur limitant dans les études en contexte canadien. La fiabilité de ces séries de données n'est pas systématiquement remise en question préalablement à leur utilisation pour des études hydrogéologiques. Il a été démontré que ceci peut avoir un impact significatif sur les estimations de la recharge. Dans cette étude, les différences entre deux séries de données météorologiques disponibles publiquement ont été quantifiées. Les écarts les plus importants proviennent des précipitations de NARR montrant une sous-estimation substantielle. Cette sous-estimation des précipitations mène inévitablement à une sous-estimation de la recharge lorsque seules les données NARR sont utilisées en valeurs d'entrées du modèle. Néanmoins, avec les mêmes valeurs de précipitation en entrée, le scénario combiné et ANUSPLIN ont tous deux montré des résultats de recharge différents. Cet écart serait dû à l'utilisation de la température comme proxy lors du calcul des termes radiatifs pour l'*PET*. Pour les régions sans mesures directes de radiation ou d'*AET*, les données NARR pourraient fournir des informations utiles au calcul de l'*PET* et la sous-estimation des précipitations pourrait différer d'un emplacement ou d'une période à l'autre considéré pour l'étude. L'interprétation des résultats comparatifs des données NARR et ANUSPLIN avec la station météorologique devrait s'effectuer avec précaution. Dans d'autres contextes, les données NARR pourraient s'avérer être de meilleure qualité que ce qui est suggéré ici. De ce fait, d'autres études effectuées au Canada ont démontré la fiabilité générale des données NARR pour la modélisation hydrogéologique.

Cette étude permet d'orienter les modélisateurs de l'eau souterraine par la mise en lumières des principaux éléments qui contrôlent la recharge et les processus se produisant dans la zone vadose en contexte québécois. La zone non saturée est bien souvent omise de nombreuses études, mais a été d'un grand intérêt dans l'étude présentée. À l'instar de tous les modèles, celui utilisé n'a pu considérer complètement tous les processus et les mécanismes se produisant dans un environnement naturel, mais la procédure peut tout de même être exportée pour la paramétrisation de modèle dans des contextes géologiques et climatiques différents. Malgré les importantes incertitudes associées à chacune des méthodes pour estimer la recharge, l'ensemble des nouvelles analyses fournissent des informations supplémentaires pour la communauté scientifique et les autorités oeuvrant dans les eaux souterraines afin de développer des stratégies plus efficaces afin d'assurer une gestion durable de la ressource.

RÉFÉRENCES

Abbaspour, K., Kasteel, R. et Schulin, R. (2000). Inverse parameter estimation in a layered unsaturated field soil. *Soil science, 165*(2), 109-123.

Allen, R. G., Pereira, L. S., Raes, D. et Smith, M. (1998). Crop evapotranspiration-Guidelines for computing crop water requirements - FAO Irrigation and drainage paper 56. *FAO, Rome, 300*(9), 56.

Assefa, K. A. et Woodbury, A. D. (2013). Transient, spatially varied groundwater recharge modeling. *Water Resources Research, 49*(8), 4593-4606.

Barbecot, F., Guillon, S., Pili, E., Larocque, M., Gibert-Brunet, E., Hélie, J.-F., Noret, A., Plain, C., Schneider, V. et Mattei, A. (2018). Using water stable isotopes in the unsaturated zone to quantify recharge in two contrasted infiltration regimes. *Vadose Zone Journal, 17*(1).

Bot, A. et Benites, J. (2005). *The importance of soil organic matter: Key to drought-resistant soil and sustained food production*. Rome : Food & Agriculture Org.

Carrera, J. et Neuman, S. P. (1986). Estimation of aquifer parameters under transient and steady state conditions: 2. Uniqueness, stability, and solution algorithms. *Water Resources Research, 22*(2), 211-227.

Choi, W., Kim, S. J., Rasmussen, P. F. et Moore, A. R. (2009). Use of the North American Regional Reanalysis for hydrological modeling in Manitoba. *Canadian Water Resources Journal, 34*(1), 17-36.

Crosbie, R. S., Binning, P. et Kalma, J. D. (2005). A time series approach to inferring groundwater recharge using the water table fluctuation method. *Water Resources Research, 41*(1).

Dean, W. E. (1974). Determination of carbonate and organic matter in calcareous sediments and sedimentary rocks by loss on ignition; comparison with other methods. *Journal of Sedimentary Research, 44*(1), 242-248.

Delin, G. N., Healy, R. W., Lorenz, D. L. et Nimmo, J. R. (2007). Comparison of local- to regional-scale estimates of ground-water recharge in Minnesota, USA. Journal of Hydrology, 334(1), 231-249.

Dripps, W. R. et Bradbury, K. R. (2007). A simple daily soil–water balance model for estimating the spatial and temporal distribution of groundwater recharge in temperate humid areas. Hydrogeology Journal, 15(3), 433-444.

Feddes, R. A., Kowalik, P. J. et Zaradny, H. (1978). Simulation of field water use and crop yield. New York, NY : Jonh Wiley & Sons.

Folk, Robert L. (1954). The distinction between grain size and mineral composition in sedimentary-rock nomenclature. The Journal of Geology 62 (4): 344-59.

Fortin, V. et Turcotte, R. (2007). *Le modèle hydrologique MOHYSE :* note de cours SCT8161. Université du Québec à Montréal, Département des sciences de la Terre et de l'atmosphère, 23 p.

Guber, A., Gish, T., Pachepsky, Y., van Genuchten, M. T., Daughtry, C., Nicholson, T. et Cady, R. (2008). Temporal stability in soil water content patterns across agricultural fields. *Catena, 73*(1), 125-133.

Healy, R. W. (2010). *Estimating groundwater recharge*. UK : Cambridge University Press.

Healy, R. W. et Cook, P. G. (2002). Using groundwater levels to estimate recharge. *Hydrogeology journal, 10*(1), 91-109.

Heiri, O., Lotter, A. F. et Lemcke, G. (2001). Loss on ignition as a method for estimating organic and carbonate content in sediments: reproducibility and comparability of results. *Journal of Paleolimnology, 25*(1), 101-110.

Hopkinson, R. F., McKenney, D. W., Milewska, E. J., Hutchinson, M. F., Papadopol, P. at Vincent, L. A. (2011). Impact of aligning climatological day on gridding daily maximum–minimum temperature and precipitation over Canada. *Journal of Applied Meteorology and Climatology, 50*(8), 1654-1665.

Hutchinson, M. F., McKenney, D. W., Lawrence, K., Pedlar, J. H., Hopkinson, R. F., Milewska, E. et Papadopol, P. (2009). Development and testing of Canada-wide interpolated spatial models of daily minimum–maximum temperature and precipitation for 1961–2003. *Journal of Applied Meteorology and Climatology, 48*(4), 725-741.

Jackson, T. J. (2002). Remote sensing of soil moisture: implications for groundwater recharge. *Hydrogeology Journal, 10*(1), 40-51.

Jacques, D., Šimůnek, J., Timmerman, A. et Feyen, J. (2002). Calibration of Richards' and convection–dispersion equations to field-scale water flow and solute transport under rainfall conditions. *Journal of Hydrology, 259*(1), 15-31.

Jiménez-Martínez, J., Skaggs, T. H., van Genuchten, M. T. et Candela, L. (2009). A root zone modeling approach to estimating groundwater recharge from irrigated areas. *Journal of Hydrology, 367*(1–2), 138-149.

Krul, W. F. J. M. et Liefrinck, F. A. (1946). Recent groundwater investigations in the Nethelands.

Langlois, A., Kohn, J., Royer, A., Cliche, P., Brucker, L., Picard, G., Fily, M., Derksen, C. et Willemet, J. (2009). Simulation of snow water equivalent (SWE) using thermodynamic snow models in Québec, Canada. *Journal of Hydrometeorology, 10*(6), 1447-1463.

Larocque, M., Meyzonnat, G., Ouellet, M. A., Graveline, M. H., Gagné, S., Barnetche, D. et Dorner, S. (2015). *Projet de connaissance des eaux souterraines de la zone de Vaudreuil-Soulanges - Rapport scientifique*. Rapport déposé au ministère du Développement durable, de l'Environnement et de la Lutte contre les Changements Climatiques. 202 p.

Loheide, S. P., Butler Jr, J. J. et Gorelick, S. M. (2005). Estimation of groundwater consumption by phreatophytes using diurnal water table fluctuations: A saturated-unsaturated flow assessment. *Water resources research, 41*(7).

Maggioni, V., Sapiano, M. R., Adler, R. F., Tian, Y. et Huffman, G. J. (2014). An error model for uncertainty quantification in high-time-resolution precipitation products. *Journal of Hydrometeorology, 15*(3), 1274-1292.

Marquardt, D. W. (1963). An Algorithm for Least-Squares Estimation of Nonlinear Parameters. *Journal of the Society for Industrial and Applied Mathematics, 11*(2), 431-441.

Martínez-Fernández, J. et Ceballos, A. (2003). Temporal stability of soil moisture in a large-field experiment in Spain. *Soil Science Society of America Journal, 67*(6), 1647-1656.

McKenna, S. A., Doherty, J. et Hart, D. B. (2003). Non-uniqueness of inverse transmissivity field calibration and predictive transport modeling. *Journal of Hydrology, 281*(4), 265-280.

McKenney, D. W., Hutchinson, M. F., Papadopol, P., Lawrence, K., Pedlar, J., Campbell, K., Milewska, E., Hopkinson, R. F., Price, D. et Owen, T. (2011). Customized spatial climate models for North America. *Bulletin of the American Meteorological Society, 92*(12), 1611-1622.

MELCC (Ministère de l'Environnement et de la Lutte contre les changements climatiques). (2019a). *Données du Programme de surveillance du climat* Québec : Direction générale du suivi de l'état de l'environnement. Récupéré de http://www.environnement.gouv.qc.ca/climat/normales/index.asp

MELCC (2019b). *Programme d'aquisition de connaissance sur les eaux souterraines*. Récupéré de http://www.environnement.gouv.qc.ca/eau/souterraines/programmes/acquisition-connaissance.htm

Mesinger, F., DiMego, G., Kalnay, E., Mitchell, K., Shafran, P. C., Ebisuzaki, W., Jović, D., Woollen, J., Rogers, E. et Berbery, E. H. (2006). North American regional reanalysis. *Bulletin of the American Meteorological Society, 87*(3), 343-360.

Min, L., Shen, Y. et Pei, H. (2015). Estimating groundwater recharge using deep vadose zone data under typical irrigated cropland in the piedmont region of the North China Plain. *Journal of Hydrology, 527*, 305-315.

Mualem, Y. (1976). A new model for predicting the hydraulic conductivity of unsaturated porous media. *Water resources research, 12*(3), 513-522.

Myneni, R., Knyazikhin, Y. et Park, T. (2015). *MCD15A3H MODIS/Terra+Aqua Leaf Area Index/FPAR 4-day L4 Global 500m SIN Grid V006* [données satellitaires]. NASA EOSDIS Land Processes DAAC.

NASA. (2017) *Quebec Flooding 2017*. Dans *NASA Earth Science Disasters Program*. Récupéré de https://disasters.nasa.gov/quebec-flooding-2017

Ouranos (2015). *Vers l'adaptation : Synthese des connaissances sur les changements climatiques au Quebec* (éd. 2015). Montreal, Quebec : Ouranos. 415 p.

Ritter, A., Hupet, F., Muñoz-Carpena, R., Lambot, S. et Vanclooster, M. (2003). Using inverse methods for estimating soil hydraulic properties from field data as an alternative to direct methods. *Agricultural Water Management, 59*(2), 77-96.

Rudolph, T. D. (1985). Jack pine (Pinus banksiana Lamb.). *Forest Service,* 252.

Scanlon, B. R., Healy, R. W. et Cook, P. G. (2002). Choosing appropriate techniques for quantifying groundwater recharge. *Hydrogeology Journal, 10*(1), 18-39.

Schaap, M. G., Leij, F. J. et van Genuchten, M. T. (2001). Rosetta: a computer program for estimating soil hydraulic parameters with hierarchical pedotransfer functions. *Journal of Hydrology, 251*(3), 163-176.

Scharnagl, B., Vrugt, J. A., Vereecken, H. et Herbst, M. (2011). Inverse modeling of in situ soil water dynamics: investigating the effect of different prior distributions of the soil hydraulic parameters. *Hydrol. Earth Syst. Sci., 15*(10), 3043-3059.

Sentelhas, P. C., Gillespie, T. J. et Santos, E. A. (2010). Evaluation of FAO Penman–Monteith and alternative methods for estimating reference evapotranspiration with missing data in Southern Ontario, Canada. *Agricultural Water Management, 97*(5), 635-644.

Shen, Y., Xiong, A., Wang, Y. et Xie, P. (2010). Performance of high-resolution satellite precipitation products over China. *Journal of Geophysical Research: Atmospheres, 115*(D2).

Šimůnek, J., van Genuchten, M. T. et Wendroth, O. (1998). Parameter estimation analysis of the evaporation method for determining soil hydraulic properties. *Soil Science Society of America Journal, 62*(4), 894-905.

Šimůnek, J., Šejna, M., Saito, H., Sakai, M. et van Genuchten, M. T. (2013). *The HYDRUS-1D Software Package for Simulating the One-Dimensional Movement of Water, Heat, and Multiple Solutes in Variably-Saturated Media, Version 4.17*. (HYDRUS Software Series 3). Riverside, Californie, USA: Department of Environmental Sciences, University of California Riverside.

Singh, J., Knapp, H. V. et Demissie, M. (2004). *Hydrologic modeling of the Iroquois River watershed using HSPF and SWAT* (ISWS CR 2004-08). Champaign, Illinois : Illinois State Water Survey.

Soil moisture Equipment Corp. (2013). *Guelph permeameter calculator spreadsheet.* Récupéré de http://www.soilmoisture.com/operating.html

Szilagyi, J., Zlotnik, V. A., Gates, J. B. et Jozsa, J. (2011). Mapping mean annual groundwater recharge in the Nebraska Sand Hills, USA. *Hydrogeology Journal, 19*(8), 1503-1513.

Thoma, M. J., Barrash, W., Cardiff, M., Bradford, J. et Mead, J. (2014). Estimating Unsaturated Hydraulic Functions for Coarse Sediment from a Field-Scale Infiltration Experiment. *Vadose Zone Journal, 13*(3).

Turkeltaub, T., Kurtzman, D., Bel, G. et Dahan, O. (2015). Examination of groundwater recharge with a calibrated/validated flow model of the deep vadose zone. *Journal of Hydrology, 522*, 618-627.

Van Genuchten, M. T. (1980). A closed-form equation for predicting the hydraulic conductivity of unsaturated soils 1. *Soil science society of America journal, 44*(5), 892-898.

von Freyberg, J., Moeck, C. et Schirmer, M. (2015). Estimation of ground water recharge and drought severity with varying model complexity. *Journal of Hydrology, 527*, 844-857.

Vrugt, J. A., Bouten, W. et Weerts, A. H. (2001). Information Content of Data for Identifying Soil Hydraulic Parameters from Outflow Experiments. *Soil Science Society of America Journal, 65*(1), 19-27.

Wang, T., Franz, T. E., Yue, W., Szilagyi, J., Zlotnik, V. A., You, J., Chen, X., Shulski, M. D. et Young, A. (2016). Feasibility analysis of using inverse modeling for estimating natural ground water recharge from a large scale soil moisture monitoring network. *Journal of Hydrology, 533*, 250-265.

Wang, T., Franz, T. E. et Zlotnik, V. A. (2014). Controls of soil hydraulic characteristics on modeling groundwater recharge under different climatic conditions. *Journal of Hydrology, 521*, 470-481.

Wang, T., Wedin, D. et Zlotnik, V. A. (2009b). Field evidence of a negative correlation between saturated hydraulic conductivity and soil carbon in a sandy soil. *Water Resources Research, 45*(7).

Weeks, E. P. (2002). The Lisse effect revisited. *Groundwater, 40*(6), 652-656.

Wollschläger, U., Pfaff, T. et Roth, K. (2009). Field-scale apparent hydraulic parameterisation obtained from TDR time series and inverse modeling. *Hydrology and Earth System Sciences, 13*(10), 1953-1966.

Wong, J. S., Razavi, S., Bonsal, B. R., Wheater, H. S. et Asong, Z. E. (2017). Inter-comparison of daily precipitation products for large-scale hydro-climatic applications over Canada. *Hydrol. Earth Syst. Sci., 21*(4), 2163-2185.

Xie, Y., Cook, P. G., Simmons, C. T., Partington, D., Crosbie, R. et Batelaan, O. (2018). Uncertainty of groundwater recharge estimated from a water and energy balance model. *Journal of Hydrology, 561*, 1081-1093.

Zha, T., Barr, A. G., van der Kamp, G., Black, T. A., McCaughey, J. H. et Flanagan, L. B. (2010). Interannual variation of evapotranspiration from forest and grassland ecosystems in western canada in relation to drought. *Agricultural and Forest Meteorology, 150*(11), 1476-1484.